A COMPARISON OF IMPEDANCE MEASUREMENT TECHNIQUES IN AIR
(U) NAVAL POSTGRADUATE SCHOOL MONTEREY CA   J T MASON
MAR 84

F/G 20/1   NL

MICROCOPY RESOLUTION TEST CHART

NATIONAL BUREAU OF STANDARDS-1963-A

NAVAL POSTGRADUATE SCHOOL
Monterey, California

THESIS

A COMPARISON OF IMPEDANCE MEASUREMENT
TECHNIQUES IN AIR

by

James Thomas Mason

March 1984

Thesis Advisors: J. L. Wayman / S. L. Garrett

84 07 30 017

REPORT DOCUMENTATION PAGE	READ INSTRUCTIONS BEFORE COMPLETING FORM

1. REPORT NUMBER	2. GOVT ACCESSION NO.	3. RECIPIENT'S CATALOG NUMBER
	AD-A143638	

4. TITLE (and Subtitle)	5. TYPE OF REPORT & PERIOD COVERED
A Comparison of Impedance Measurement Techniques in Air	Master's Thesis March, 1984
	6. PERFORMING ORG. REPORT NUMBER

7. AUTHOR(s)	8. CONTRACT OR GRANT NUMBER(s)
James Thomas Mason	

9. PERFORMING ORGANIZATION NAME AND ADDRESS	10. PROGRAM ELEMENT, PROJECT, TASK AREA & WORK UNIT NUMBERS
Naval Postgraduate School Monterey, California 93943	

11. CONTROLLING OFFICE NAME AND ADDRESS	12. REPORT DATE
Naval Postgraduate School Monterey, California 93943	March 1984
	13. NUMBER OF PAGES
	91

14. MONITORING AGENCY NAME & ADDRESS(If different from Controlling Office)	15. SECURITY CLASS. (of this report)
	15a. DECLASSIFICATION/DOWNGRADING SCHEDULE

16. DISTRIBUTION STATEMENT (of this Report)

Approved for Public Release; Distribution Unlimited

17. DISTRIBUTION STATEMENT (of the abstract entered in Block 20, if different from Report)

18. SUPPLEMENTARY NOTES

19. KEY WORDS (Continue on reverse side if necessary and identify by block number)

Acoustic Impedance, Impedance Measurements, Standing Wave Tube, Dual-Microphone Technique, Helmholtz Resonators

20. ABSTRACT (Continue on reverse side if necessary and identify by block number)

The acoustic impedance of several Helmholtz resonators were measured using two different techniques. The first technique employed the conventional Standing Wave Tube method. The second was the Dual-Microphone Transfer Function of J.Y. Chung and D.A. Blaser. The calculability of the frequency dependent Helmholtz resonator impedance allowed the methods to be compared for both absolute accuracy and relative precision. The average relative precision for the SWT technique was 4.2% while the average for the dual-microphone technique was 18.4%.

DD FORM 1473 EDITION OF 1 NOV 65 IS OBSOLETE
1 JAN 73

S/N 0102-LF-014-6601

1

A Comparison of Impedance Measurement
Techniques in Air

by

James Thomas Mason
Lieutenant Commander, United States Navy
B.S., United States Naval Academy, 1970

Submitted in partial fulfillment of the
requirements for the degree of

MASTER OF SCIENCE IN ENGINEERING ACOUSTICS

from the

NAVAL POSTGRADUATE SCHOOL
March 1984

Author: _____

Approved by: _____
                                        Thesis Advisor

_____
                                        Co-Advisor

_____
Chairman, Engineering Acoustics Curriculum Committee

_____
                        Dean of Science and Engineering

2

ABSTRACT

The acoustic impedance of several Helmholtz resonators were measured using two different techniques. The first technique employed the conventional Standing Wave Tube method. The second was the Dual-Microphone Transfer Function method of J.Y. Chung and D.A. Blaser. The calculability of the frequency dependent Helmholtz resonator impedance allowed the methods to be compared for both absolute accuracy and relative precision. The average relative precision for the SWT technique was 4.2% while the average for the dual-microphone technique was 18.4%.

3

TABLE OF CONTENTS

LIST OF TABLES

LIST OF FIGURES

7

8

I. INTRODUCTION

Acoustic impedance tubes have been used for many years to obtain complex accustic impedances, reflection coefficients and phase information for many different types of materials. The techniques used with the impedance tubes have been many and varied. This study involves the comparison of the dual-microphone transfer function technique used by Chung and Blaser [Ref. 1] and the standing wave tube (SWT) technique to determine their absolute accuracy and relative precision. This work was undertaken as a prelude to the extension of computer controlled impedance measurement techniques to water.

A. IMPEDANCE MEASUREMENT TECHNIQUES

Many different impedance measurement techniques have been used over the years. Beranek [Ref. 2] divides the different techniques into three general categories, Surface Methods, Transmission Line Methods and Comparison Methods. This study looked closely at only two of the techniques, however, some of the other methods are worth mentioning as background.

1. Surface Methods

These methods involve the measurement of the sound pressure at a point on the surface of interest and the particle or volume velocity at the surface. Cook [Ref. 3] did this using a short tube of a given radius and length and a clamped-edge diaphram. He was then able to calculate the volume velocity and the average pressure over the surface of the sample. Beranek [Ref. 4] presented a useful theory for

9

predicting the normal acoustic impedance of porous materials in terms of their flow resistance, porosity and effective dynamic mass of the enclosed gas.

2. Transmission Line Methods

By far, the most popular methods of impedance measurements fall into this category. The standing wave tube and dual-microphone techniques in this study are included. They will be examined in detail later. Another technique involves the measurement of the pressure-frequency resonance curve and determining the curve width and resonant frequency. Harris [Ref. 5] [Ref. 6] discusses two of these methods which are closely related to each other.

Finally, one additional method currently in use by the U.S. Navy for making acoustical measurements deserves mentioning. [Ref. 7] This system is digital and is used for underwater acoustical measurements from 1 Hz. to approximately 2 MHz. This digital measuring system employes a buffered video analog-to-digital converter and was primarily designed to perform acoustical measurements using the Prony Method. [Ref. 8] [Ref. 9] The system uses a stable signal and sampling source and 12-bit, 5 MHz., analog-to-digital converter with a 4K buffer memory. A PDP-11/23 serves as a controller as well as a signal processor for averaging and amplitude and phase estimation.

3. Comparison Methods

These methods mainly involve the use of acoustical bridges or reliable acoustical standards. Steward first introduced [Ref. 10] the simplest and most rapid to use. Later refinements followed [Ref. 11] but suitable variable standards of acoustical resistance and reactance were difficult to obtain. The use of reliable acoustic standards, rigid wall and an eighth-wavelength tube, was reported by

10

Flanders [Ref. 12] in 1932. However, mathematical calculations were difficult.

In this study, the transmission line method and the comparison method are combined by introducing a new "standard", the Helmholtz resonator. This standard has the advantage of having an easily calculable reactance which is absolute to within one adjustable parameter. This parameter is fixed by the Helmholtz resonance frequency which is easily measured to a high degree of precision and absolute accuracy.

B. HISTORY OF DUAL-MICROPHONE MEASURING TECHNIQUES

Clapp and Firestone [Ref. 13] first mentioned the use of two microphones in an article published in 1941. In this article it was recognized that their equipment could be used to measure the absorption coefficient of materials. Later, Shultz [Ref. 14] published an article on the acoustic wattmeter and its application for measuring absorption coefficients. During this time the use of the acoustic wattmeter for impedance measurements was little used since the standing wave tube (SWT) technique was the most favored method.

In 1977 Seybert and Ross [Ref. 15] published an article which discussed an experimental technique using two microphones and random noise excitation. This technique used digital methods and the auto- and cross-spectra to determine the normal complex reflection coefficient of a sample terminating a tube. Finally, in 1980, Chung and Blaser [Ref. 1] published their article discussing the transfer function technique for measuring in-duct acoustic properties. This technique also used digital methods and the auto- and cross-spectra to determine the normal complex reflection coefficient. However, the mathematics did not involve the

matrix-inversion used by Seybert and Ross and as a result the computation time was significantly reduced.

A two microphone technique utilizing pure tone rather than random excitation and analog rather than digital processing is described by Elliot. [Ref. 16]

C. PURPOSE OF STUDY

The above methods have been used to measure numerous materials of differing acoustic properties. However, the properties of these materials were not known or calculable to any reasonable accuracy. The aim of this study was to determine the absolute accuracy of the dual-microphone technique and its relative precision compared to the SWT technique as a prelude to the development of an impedance measurement apparatus for use in water. A Helkholtz resonator was used to accomplish this comparison.

II. COMPARISON OF MEASUREMENT TECHNIQUES

Previous studies of impedance measurement techniques involved the use of materials for which the impedance was not accurately known. This study deals with impedance measurements using a Helmholtz resonator as a calculable standard to determine the absolute accuracy and relative precision of the two techniques. A Helmholtz resonator was chosen because its various acoustical parameters could be independently measured or calculated and then compared to the experimental results.

A. THEORETICAL BACKGROUND

The term "acoustic impedance" can have different meanings for different situations. It is necessary to define exactly the different impedances involved in this study. This is necessary to prevent confusion later when the relationship between the different impedances is used to determine the calculated acoustical properties of a Helmholtz resonator. Normally this is not necessary since the specific acoustic impedance and the acoustic impedance differ by a constant with the dimensions of area.

1. Specific Acoustic Impedance

The specific accustic impedance is defined as the ratio of acoustic pressure in a medium to the associated Eulerian particle speed. [Ref. 17]

$$Z_s = p/u \qquad (2.1)$$

The MKS unit of specific acoustic impedance is Pa-s/m.

The specific acoustic impedance of a medium is a real quantity for plane waves. However, this not true for the standing waves generated in an impedance tube. For this case, the specific acoustic impedance will be complex and can expressed in the form

$$Z_s = r + jx \qquad (2.2)$$

where "r" is the specific acoustic resistance and "x" is the specific acoustic reactance for the medium concerned.

2. Acoustic Impedance

The acoustic impedance of a medium acting on a surface of area "A" is the ratio of the acoustic pressure at the surface to the volume velocity at the surface [Ref. 17]

$$Z_a = p/U \qquad (2.3)$$

where $U = uA$ if u is normal to the surface of area "A". The MKS unit of acoustic impedance is Pa-s/m^3, which is also termed an acoustic ohm. The acoustic impedance and the specific acoustic impedance are related at the surface of area "A" by

$$Z_a = Z_s/A \qquad (2.4)$$

3. Mechanical Impedance

The mechanical impedance is the ratio of the driving force to the resultant particle speed at the point where the force is applied [Ref. 17]

$$Z_m = F/u \qquad (2.5)$$

The MKS unit of mechanical impedance is N-s/m, also referred to as a mechanical ohm.

14

4. Helmholtz Resonator

A Helmholtz resonator can be treated as a lumped parameter system. The resonator consists of a volume "V" with rigid walls and a neck of length "L" and cross-sectional area "A". The acoustic pressure in the volume provides the lumped stiffness "s" if the wavelength is much greater than the cube root of the volume. The fluid in the neck provides the lumped mass as long as the wavelength is much greater than the length of the neck. Finally, the resistance is provided by the opening radiating sound, if the wavelength is much greater than the square root of the cross-sectional area of the neck. An additional resistance is introduced by viscous losses in the neck and irreversible thermal conduction to the volume boundries if the compression of the gas is adiabatic and the walls remain isothermal. However, since these resistance sources are not easily calculated from "First Principles", they are neglected. The radiation resistance "R " can be calculated, however, its value is dependent upon the impedance of the medium which changes. To get the viscous loss resistance term the flow field in the neck is required. Therefore these resistance terms are of little use in this calculation.

The fluid in the neck has an effective mass given by [Ref. 17]

$$m = \rho A L' \tag{2.6}$$

where "L' " is the effective length of the neck and is a function of actual length "L" and the neck radius "a" and the flow field in the vicinity of the oriface. The effective mass is greater than the actual mass in the neck due the radiation-mass loading at the ends generated by this extended flow field. The stiffness of the resonator is given by [Ref. 17]

$$s = (\rho c^2)(A^2)/V \tag{2.7}$$

15

By driving the Helmholtz resonator with a sound wave of pressure amplitude "P", the following equation for the inward displacement "x" of the fluid in the neck results [Ref. 17]

$$m\frac{d^2x}{dt^2} + R_r\frac{dx}{dt} + sx = APe^{j\omega t} \qquad (2.8)$$

This differental equation is the same as that for a driven oscillator and the mechanical impedance of the Helmholtz resonator can be expressed as [Ref. 17]

$$Z_m = R_r + j(\omega m - s/\omega) \qquad (2.9)$$

where the mechanical reactance "X_m" is given by

$$X_m = \omega m - s/\omega \qquad (2.10)$$

Since the resonance occurs when $X_m = 0$, the resonant frequency "ω_o" follows

$$\omega_o^2 = s/m \qquad (2.11)$$

Using equations (2.6) and (2.7)

$$\omega_o^2 = \frac{\rho c A^2}{V \rho A L'}$$

The final result obtained from cancelling terms is

$$\omega_o = c\sqrt{\frac{A}{VL'}} \qquad (2.12)$$

It should be noted that nowhere in the derivarion of equation (2.12) is any restriction placed on the physical arrangement of the Helmholtz resonator. Figure 2.1 shows the arrangement used for this study. As can be seen from

equation (2.12) and the figure, the resonant frequency can be changed by changing the area of "neck"(diameter D_i), the volume of the resonator (change depth h) or the length of the "neck"(thickness t).

Recalling equation (2.10)

$$X_m = \omega m - s/\omega \tag{2.10}$$

and by factoring out "m" and using equation (2.11), the following result is obtained

$$X_m = m(\omega - \omega_o^2/\omega)$$

Since $\omega = 2\pi f$ the final form is obtained

$$X_m = 2\pi m(f - f_o^2/f)$$

where f is the frequency in hertz. For convenience we define

$$X_m' = f - f_o^2/f \tag{2.13}$$

so that

$$X_m = 2\pi m X_m' \tag{2.14}$$

It is now possible to derive the relationship between the specific acoustic reactance "X_s" and "X_m'". Given a resonator as shown in Figure 2.2, divided into sections 1 and 2 as indicated and recalling equation (2.1)

$$Z_s = p_1/u_1 \tag{2.15}$$

where p_1 and u_1 represent the pressure and particle speed, respectively, in section 1. This is the specific acoustic impedance of the medium in section 1.

Next using equation (2.5)

$$Z_m = P_2/u_2 \tag{2.16}$$

Converting P_2 to a pressure at the boundary results in

17

$$Z_m = \frac{p_2 A_2}{u_2} \qquad (2.17)$$

where p_2 and u_2 represent the pressure and particle speed, respectively, in section 2. A_2 is the cross-sectional area of the resonator neck. Since there is no physical boundary between sections 1 and 2, the pressures on both sides must be equal.

$$p_1 = p_2 = p$$

Also, the volume velocities must be equal across the boundry. Therefore

$$A_1 u_1 = A_2 u_2$$

$$u_2 = \frac{A_1}{A_2} u_1 \qquad (2.18)$$

Substituting equation (2.18) into equation (2.17) and regrouping the appropriate terms results in

$$Z_m = (\frac{p}{u_1})(\frac{A_1^2}{A_2}) \qquad (2.19)$$

Finally, it can be seen that the quantity (p/u_1) is just the specific accustic impedance and the result is

$$\frac{Z_s}{Z_m} = \frac{A_2}{A_1^2} \qquad (2.20)$$

Since the impedances are composed of the resistive and reactive parts, the reactive portions vary in the same manner. Therefore,

$$\frac{X_s}{X_m} = \frac{A_2}{A_1^2} \qquad (2.21)$$

18

It can be seen from equation (2.14) that

$$-\frac{X_s}{X_m} = 2\pi m - \frac{X_s}{X_m} -$$

It should be noted that the two techniques in this study provide the values for specific acoustic impedance normalized to the characteristic impedance "ρc". Therefore, the preceding equation becomes

$$\frac{X_s/\rho c}{X_m'} = 2\pi m - \frac{X_s/\rho c}{X_m}$$

and, finally, substituting for "m" from equation (2.6) and for "X_s/X_m" from equation (2.21)

$$\frac{X_s/\rho c}{X_m} = \frac{2\pi L' A_1}{c A_2} --- \tag{2.22}$$

As can be seen, this equation does not depend on frequency and therefore remains constant as frequency changes. For convenience this constant is called "K_{th}" with the subscript signifying the theoretical value for the ratio of "$X_s/\rho c X_m'$" for a given Helmholtz resonator.

$$K_{th} = \frac{2\pi L' A_1}{c A_2} ----- \tag{2.23}$$

"K_{th}" has been reduced to an expression which contains only directly measurable terms with the exception of "L'", the effective length of the neck. However, by using equation (2.12) "L'" can be determined from parameters which are measurable by separate means. Later in this chapter, "L'" will be looked at more closely for comparison with the

19

calculated "L'" for other Helmholtz resonator configurations.

B. STANDING WAVE TUBE TECHNIQUE (SWT)

The standing wave tube technique provides a convenient laboratory method for determining the absorption coefficient and specific acoustic impedance of materials. The method, however, is somewhat tedious when a large number of samples is measured or measurements of a single sample are required at a great number of frequencies.

1. Theory

The sample to be measured is placed at one end of the standing wave tube. At the other is mounted a loud-speaker. A microphone probe is inserted through the loud-speaker end and is attached to a microphone car. The car moves such that the microphone probe is moved along the axis of the tube.

A pure tone signal is reflected from the sample. The reflected wave interferes with the incident wave and a standing wave is established. The microphone probe and car arrangement allows for the location and acoustic pressure of the nodes and anti-nodes to be measured. From the measurement of these amplitude and phase characteristics, calculation of absorption coefficient and specific acoustic impedance of a sample is possible.

From reference 6, the following are the equations needed for the determination of the desired acoustic parameters.

$$\frac{X}{\rho c} = \frac{Tan\,\psi_2(1 - Tanh^2\,\psi_1)}{Tanh^2\,\psi_1 + Tan^2\,\psi_2} \qquad (2.24)$$

where

$$\psi_1 = \coth^{-1}\left[-\frac{P_{max}}{P_{min}}-\right] \qquad (2.25)$$

and

$$\psi_2 = \frac{\pi}{2}\left[1 - -\frac{4d}{\lambda}--\right] \qquad (2.26)$$

"P_{max}" and "P_{min}" are the maximum and minimum pressures in the standing wave tube and "d" is the distance to the first pressure minimum (node) from the sample. (NOTE: The microphone output voltage is the actual measurement made since only the ratio of the pressures is required)

2. Equipment Set-up

Figure 2.3 is a simplified representation of the equipment used in the standing wave tube technique. It includes the Bruel and Kjaer Standing Wave Apparatus Type 4002, a HP 302A Wave Analyzer and an amplifier and frequency counter.

a. Bruel and Kjaer Type 4002 Standing Wave Apparatus

The apparatus is designed for easy and quick evaluation of acoustic materials by the standing wave method. A major advantage is that relatively small circular samples (10 cm. in diameter) are all that are required.

The tube used had an interior diameter of 10 cm., which covered a frequency range of 90 to 1800 hz. The lower limit was set by the length of the tube and the upper limit determined by the cut-off frequency for the lowest non-plane wavemode of the tube. [Ref. 18] Two sample holders were also used with fixed depths of 1 in. and 2 in., respectively. The bases of the holders were very thick to present as rigid a termination as possible.

21

The microphone in the microphone car is a small dynamic microphone of adequate frequency range for the standing wave tube method. It is isolated by elastic supports in the car to reduce the effects of external airborne noise and impact sound or vibration.

b. Hewlett-Packard HP 302A Wave Analyzer

The Hewlett-Packard model 302A wave analyzer is a tunable voltmeter of high sensitivity over the frequency range of 20 Hz. to 50 kHz. The wave analyzer in the BFO mode of operation becomes an audio signal generator combined with a tuned voltmeter. Further, since the tuned voltmeter has a very narrow pass band (6 Hz), noise and harmonics of the signal have very little effect on the voltmeter reading.

3. Experimental Procedures

The standing wave tube technique was used in several different experiments. It was used with a rigid end as the sample to measure the "acoustic" end of the microphone probe tube and the sound speed. It was also used to determine the resonant frequency and reactive impedance of three Helmholtz resonators. Table I shows the physical dimensions of each of the resonators.

a. Data Collection

In all of the experiments the data was collected in the same manner. However, in the first experiment (rigid end) the only data collected was the location of the first two nodes and the frequency of the signal. Table II shows this data.

For the experiments involving the Helmholtz resonators the values of the maximum and minimum microphone output voltages were obtained in addition to the frequency and node locations. This data was placed in Tables III-V

22

TABLE I
Helmholtz Resonator Physical Dimensions

Resonator no.	Volmue cm.	Neck Diameter cm.	Neck Length cm.
1	195.52	2.52	1.27
2	381.01	2.52	1.27
3	195.52	3.46	1.00

b. Data Reduction

In the first experiment, the measured distance between the two nodes was used to calculate the wavelength. From this, the quarter-wavelength was determined and compared to the distance from the sample to the first node as measured by the microphone car. Since the "sample" was a rigid end located 5.00 cm. from the measured end of the tube, the two distances should have differed by 5 cm. Additionally, the wavelength and the frequency were used to calculate the sound speed in the tube for each frequency measured. These results are shown in Table II The average value of " d" suggests that the "acoustic center" of the probe tube is 1.7 $\pm$ .5 mm. ahead of the physical end of the probe tube over the frequency range examined.

For the experiments involving the Helmholtz resonators, the reduction of the data was somewhat different. The wavelength was determined by one of two methods depending upon whether two node locations were

TABLE II

Standing Wave Tube Sound Speed Data

Freq.	First Min.	Sec. Min.	($\lambda/4$)	Δd	c
Hz.	cm.	cm.	cm.	cm.	cm./s.
299	23.90	81.74	28.93	5.03	34588
400	16.80	59.95	21.58	4.78	34520
600	9.58	38.38	14.40	4.82	34560
800	5.96	27.53	10.78	4.79	34512
1001	3.84	21.03	8.60	4.76	34414
1197	2.19	16.91	7.35	5.16	35240
1402	1.40	13.64	6.13	4.73	34321
1599	0.54	11.36	5.40	4.86	34602
			average	4.87	34595
			deviation	.150	277
			per cent	03.08	0.80

measurable. In those cases where two or more node locations were measurable, the distance between them was used to calculate the wavelength. At the lower frequencies where only one node was measurable, the wavelength was determined from the frequency and the average sound speed found during the experiment. It should be noted that an attempt was made to use the location of the measurable anti-node to determine wavelength. However, this measurement was too inaccurate due to the nature of the waveform being measured. At the maximum, the values of amplitude are changing very slowly (second order) so that the measurement of the exact location of the maximum was very difficult. On the other hand, at the nodes, the values were changing more rapidly (first order) and the location could be easily and precisely determined.

TABLE III

Standing Wave Tube Measured Data - Resonator #1

Freq. Hz.	First Min. cm.	uv.	Sec. Min. cm.	uv.	Third Min. cm.	uv.	Maximum mv.
250	31.75	65					2.20
350	20.85	50	69.70	60			1.30
400	16.65	260	59.69	260			4.80
450	12.30	140	50.40	130	89.20	175	1.80
500	6.70	450	41.20	460	76.30	520	2.80
550	1.70	240	30.35	290	61.65	190	1.60
600	.55	200	22.50	180	51.30	185	1.78
650	.10	200	18.42	140	45.10	165	2.60
700			15.90	34	40.64	31	1.00
750			14.20	90	37.15	100	5.20
1000			9.75	30	27.15	20	3.40
1250			7.60	5	21.40	5	1.95
1500			6.75	25	17.80	5	2.50

TABLE IV

Standing Wave Tube Measured Data - Resonator #2

Freq. Hz.	First Min. cm.	uv.	Sec. Min. cm.	uv.	Third Min. cm.	uv.	Maximum mv.
250	27.88	1750					22.1
300	19.69	335	76.72	330			2.90
350	10.12	1610	59.32	1870			8.45
375	3.65	1280	49.63	1510			6.70
400	1.59	800	40.94	915	84.65	355	4.35
450	.43	480	29.90	615	68.58	565	8.00
500	0.00	164	23.96	75	58.64	128	2.88
750	13.53	24	36.35	52	59.50	38	2.91
1000	9.75	13	26.96	15	44.33	39	2.43
1250	7.44	24	21.71	43	35.12	88	2.00
1500	6.32	30	17.93	10	29.37	42	4.42

TABLE V

Standing Wave Tube Measured Data - Resonator #2

Freq.	First Min.		Sec. Min.		Third Min.		Maximum
Hz.	cm.	mv.	cm.	mv.	cm.	mv.	mv.
200	41.61	3.20					51.5
250	31.74	29.5					53.7
300	26.20	2.90	83.95	3.15			55.5
350	21.51	3.90	70.04	3.30			65.5
400	18.42	10.0	61.49	9.40			178
450	16.17	1.52	54.44	1.70			26
500	14.26	4.05	48.19	3.40	82.21	4.05	61.5
550	11.10	5.40	42.92	5.30	73.68	5.60	68.5
600	9.18	2.05	37.66	1.98	66.69	1.70	24.0
650	6.43	6.05	32.79	6.15	60.39	6.10	46.2
700	4.28	4.00	28.62	3.95	52.94	3.80	26.3
750	2.29	2.90	24.54	2.55	47.49	2.64	15.4
800	19.07	3.95	40.41	4.25	62.37	4.15	27.3
850	16.52	1.10	37.32	1.12	57.42	1.10	10.3
900	14.41	3.10	33.30	2.90	52.80	3.20	47.5
1000	11.67	.80	29.00	.90	46.18	.76	22.5
1250	8.22	.60	21.86	.45	36.08	.52	24.6
1500	6.53	.65	17.96	1.40	29.49	1.13	60.5

After the wavelength was determined, it was used
to scale the distance to the first node (Table VI). These
values were plotted versus the frequency (Figures 2.4-2.6).
The first two points above resonance were also plotted as

$$d/\lambda - .5 \tag{2.27}$$

A linear regression was then used with the two data points
both above and below resonance to determine the resonant
frequency "f". The resonant frequency for each resonator is
also shown on Figures 2.4-2.6.

Once the resonant frequency was obtained, "X_m'"
was calculated for each frequency using equation (2.13). "$X_s/\rho c$" was then calculated using equations (2.24-2.26).
Finally, the ratio of "$X_s/\rho c$" to "X_m'" (K_{exp}) was calculated
for comparison to the theoretical value (K_{th}) determined from

26

TABLE VI

Standing Wave Tube d/λ Data

Freq. Hz.	Resonator #1 d/λ	Resonator #2 d/λ	Resonator #3 d/λ
200			.2416
250	.2437	.2015	.2303
300	.2201	.1726	.2268
350	.2134	.1028	.2214
375		.0397	
400	.1934	.4683 (-.0317)	.2138
450	.1585	.3865 (-.1135)	.2113
500	.0954	.3454	.2099
550	.4848 (-.0152)		.1774
600	.3906 (-.1094)		.1596
650	.3452		.1192
700	.3213		.0880
750	.3094	.2943	.0507
800			.4404 (-.0596)
850			.4039 (-.0961)
900			.3754
1000	.2802	.2820	.3382
1250	.2754	.2688	.2950
1500	.2706	.2751	.2844

equation (2.23). Tables VII-IX list the experimental values for each Helmholtz resonator.

c. Error Analysis

Before an analysis of the errors could be attempted, it was necessary to identify all of the sources of the errors. The errors were a result of the measurements of the voltage (P_{max} and P_{min}), frequency and distances to the nodes.

Recalling equation (2.25)

$$\Psi_i = \coth^{-1} \left(-\frac{P_{max}}{P_{min}} - \right) \qquad (2.25)$$

it can be seen that for the values of "P_{max}" and "P_{min}" involved, SWR is small and therefore, an error in the standing wave ratio (SWR = $\frac{P_{max}}{P_{min}}$) has little effect on the overall calculations.

Looking at equation (2.24)

$$-\frac{X_s}{\rho c} = \frac{Tan\,\psi_2(1 - Tanh^2\,\psi_1)}{Tanh^2\,\psi_1 + Tan^2\,\psi_2} \qquad (2.24)$$

and taking into account that "ψ_1" is small, equation (2.24) then reduces to

$$-\frac{X_s}{\rho c} \approx \frac{Tan\,\psi_2}{Tan^2\,\psi_2}$$

28

TABLE VIII

Standing Wave Tube Reduced Data - Resonator #2

$$f_o = 387.8 \text{ Hz.}$$

Frequency	c	$X_s/\rho c$	X'_m	K_{exp}
Hz.	cm./s.	Pa-s/m	s^{-1}	x 10^{-3}
200	34392*	-3.86	-551.9	6.99
250	34430*	-2.43	-351.6	6.91
300	34542	-1.46	-201.3	7.25
350	34447	-.563	-79.69	7.06
375	33563*	-.070	-26.04	2.69*
400	34296	.258	24.03	10.74*
450	33516	.745	115.8	6.43
500	34620	1.55	199.2	7.78
550	34557	2.08	276.6	7.52
600	34398	2.35	349.4	6.73
650	34437	2.80	418.6	6.69
700	34503	3.23	485.2	6.66
750	34508	3.72	549.5	6.77
1000	34560	5.49	849.6	6.46
1250	34913	8.51	1130	7.53*
1500	34470	7.11	1400	5.08*
average	34444		average	6.94
deviation	314		deviation	.41
per cent	.91		per cent	5.9

*Values not used for the calculation of the average.

or

$$-\frac{X_s}{\rho c} \approx \cot \psi_2$$

away from resonance.

On the basis of this result, it was determined that the best data was obtained in the regions just away from resonance for the following reasons. First, since tan goes to zero at resonance, "ψ_2" terms begin to dominate and the errors in "ψ_1" become large when compared to "ψ_2".

29

```
                        TABLE IX
        Standing Wave Tube Reduced Data - Resonator #3

                       f_o = 773.0 Hz.
```

Frequency	c	$X_s \angle \rho c$	X'_m	K_{exp}
Hz.	cm./s.	Pa-s/m	s^{-1}	x 10^{-3}
200		-7.86	-2788	2.81
250		-6.93	-2140	3.24
300	34650	-5.72	-1692	3.38
350	33999	-5.03	-1357	3.71
400	34456	-4.09	-1094	3.74
450	34443	-3.78	- 878	4.31
500	33975	-3.63	- 695	5.22*
550	34419	-2.07	- 536	3.86
600	34506	-1.50	- 396	3.79
650	35074	-.870	- 269	3.23
700	34062	-.600	- 154	3.90
750	33900	-.313	- 46.7	6.70*
800	34640	.427	53.1	8.04*
850	34765	.616	147	4.19
900	34551	1.06	236	4.49
1000	34510	1.58	402	3.93
1250	34825	3.97	772	5.14
1500	34440	4.69	1102	4.26
average	34451		average	3.74
deviation	327		deviation	.47
per cent	.95		per cent	12.6

*Values not used for the calculation of the average.

Secondly, as the frequency gets further from resonance the cotangent function gets larger and the errors also get larger. It was for these reasons that some of the data in Tables VII-IX were deleted for the calculation of the averages.

This completes the discussion of the standing wave tube technique. The final results will be examined later in this chapter along with those for the Chung-Blaser dual-microphone technique. One additional experimental technique needs addressing. The resonant frequency of each

Helmholtz resonator was measured independently of either method. This was done using a signal generator and speaker to excite the resonators. Using a small microphone in the resonators to detect the pressure changes, the signal generator was tuned to the frequency which resulted in the greatest pressure in the resonators. These resonant frequencies were 549.5 Hz. for resonator 1, 398.5 Hz. for resonator 2 and 795.0 Hz. for resonator 3.

C. CHUNG-BLASER DUAL-MICROPHONE TECHNIQUE

The dual-microphone technique developed by Chung and Blaser provides a quick method for measuring the acoustic impedance and reflection coefficient in the laboratory. However, as will be shown later, the technique suffers some degradation in accuracy compared with the results obtained by the SWT method.

1. Theory

Chung and Blaser have shown [Ref. 1] that the complex reflection coefficients at the two microphone locations can be expressed in terms of the transfer functions of the incident and reflected waves. This expression is

$$\frac{R_1(f)}{R_2(f)} = \frac{H_i(f)}{H_r(f)} \tag{2.28}$$

where $R_1(f)$ and $R_2(f)$ are the complex reflection coefficients evaluated at the first and second microphone locations, respectively. $H_i(f)$ and $H_r(f)$ are the acoustic transfer functions associated with the incident and reflected wave components, respectively, evaluated at the two microphone locations.

31

For plane wave propagation (no mean flow) and neglecting wall losses, $H_i(f)$ and $H_r(f)$ can be expressed as

$$H_i(f) = e^{-jks} \qquad (2.29)$$

and

$$H_r(f) = e^{jks} \qquad (2.30)$$

where "k" is the wavenumber and "s" is the microphone spacing.

Application of equation (2.28) results in the reflection coefficient "R" on the surface of a sample material not at a microphone location being expressed as

$$\frac{R_l}{R} = \frac{H_i'}{H_r'} \qquad (2.31)$$

where

$$H_i' = e^{-jkl} \qquad (2.32)$$

and

$$H_r' = e^{jkl} \qquad (2.33)$$

and "1" is the distance from the first microphone to the surface of the sample material. Using equations (2.31-2.33), the reflection coefficient at the sample is

$$R = R_l \, e^{j2kl} \qquad (2.34)$$

where [Ref. 1]

$$R_l = \frac{H_{l2}(f) - H_i(f)}{H_r(f) - H_{l2}(f)} \qquad (2.35)$$

$H_{l2}(f)$ is the acoustic transfer function between microphones 1 and 2 and $H_i(f)$ and $H_r(f)$ are the transfer functions of

the incident and reflected waves, respectively, between the two microphone locations.

Using the standard relation between reflection coefficient and complex specific acoustic impedance

$$-\frac{z_s}{\rho c}- = \frac{(1+R)}{(1-R)}$$ (2.36)

and the relationships in equations (2.34) and (2.35), the complex specific acoustic impedance can be determined at a distance "l" from the first microphone [Ref. 1]

$$-\frac{z_s}{\rho c}- = j \frac{H_{12}\sin(kl) - \sin[k(l-s)]}{\cos[k(l-s)] - H_{12}\cos(kl)} ----------------$$ (2.37)

where

$$-\frac{X_s}{\rho c}- = \frac{Re(H_{12})\sin[k(l-s)] - \frac{1}{2}\{\sin[2k(l-s)] + |H_{12}|^2\sin(2kl)\}}{\cos^2[k(l-s)] - [2Re(H_{12})\cos(kl)][\cos[k(l-s)]] + |H_{12}|^2\cos^2(kl)}$$ (2.38)

$H_{12}(f)$ can be expressed as

$$H_{12}(f) = \frac{C_{12} + jQ_{12}}{S_{11}(f)}----$$ (2.39)

where C_{12} and Q_{12} are the real and imaginary parts of the cross-power spectrum of the signals at microphones 1 and 2. $S_{11}(f)$ is the auto-power spectrum of the signals at microphone 1.

Finally, Seybert and Ross show [Ref. 15] that the phase change upon reflection is given by

$$\phi(f) = \tan^{-1}\left[-\frac{Q_{ir}(f)}{C_{ir}(f)}-\right]$$ (2.40)

33

where Q_{ir} and C_{ir} are the imaginary and real parts of the cross-power spectrum of the incident to reflected waves.

2. Equipment Set-up

Figure 2.7 shows a simplified diagram of the Chung-Blaser dual-microphone technique equipment set-up. At the center of the system are the Hewlett-Packard HP-85 computer and HP-5420 Signal Analyzer System.

a. The Hewlett-Packard HP-85 Computer

The HP-85 computer is an 8 bit microprocessor which uses the BASIC computer language. It has 16K bytes of read/write memory of which 14,579 bytes are available for use by the operator. The unit used in the study had its memory expanded to 32K bytes by a memory module. The unit has a mass storage capability in the form of a magnetic tape reader/recorder. It also includes a 127 millimeter diagonal black and white electromagnetic deflection CRT and a 32 character per line thermal printer/plotter. To interface with other equipment, an I/O ROM and interface card were added to provide HP-IE (IEEE-488) interface capability.

b. The Hewlett-Packard HP-5420 Signal Analyzer

The Hewlett-Packard HP-5420A Signal Analyzer provides digital time-domain and frequency-domain analysis of low frequency analog signals. The HP-5420A system includes the HP-5447B Digital Filter Module, HP-54410A Analog to Digital Converter, HP-5443A Keyboard and Control Module and the 5441A Display Module. The equipment used in this study also included an HP-10920A HP-IB interface accessory. This allowed its use with an HP-IB controller. It allowed the transfer of data and measurement set-up information to pass to and from the controller and allowed the reception of remote control commands. Using the controller,

34

the data was modified, processed, saved and recalled resulting in a high degree of flexibility.

The HP-5420A Signal Analyzer performes a variety of time-domain and frequency-domain measurements. All measurements are done using digital signal processing. This involves filtering and sampling the input waveforms. The analog input is first filtered by a low-pass filter and then passed to an analog to digital converter. Here, the waveform is sampled which results in the conversion of a voltage (at a certain point in time) into a numerical representation. These numbers are then filtered and processed digitally to produce the various measurements preformed by the analyzer.

c. The Impedance Measurement Tube

The tube used in this part of the study was a piece of 3 inch inside diameter PVC pipe 12 inches long with a 3 inch loudspeaker mounted at one end. Two holes were drilled in the tube and fitted with 7/8 inch Tygon tubing to hold the two microphones. The first was located 11.42 cm. from the sample end (opposite the loudspeaker) and the second was located 4.59 cm. from the first. The distances were measured to the center of the microphones.

The microphones used were General Radio 1962 1/2 inch electret-condenser microphones. These microphones have a sensitivity level of -40 dB re 1 v/Pa and have typically flat response curves from 20 Hz. out to 1800 Hz. which cover the frequency range of the study.

3. Experimental Procedures

The dual-microphone technique was used to determine the resonant frequency and the reactive impedance of the same three Helmholtz resonators used with the standing wave tube technique. A major difference between the two techniques made itself known almost immediately. The time to collect and reduce the data was vastly different.

35

a. Microphone Calibration

The two microphone/preamplifier channels had to be calibrated for phase and amplitude differences prior to use for the actual measurements. The technique used for this calibration was to place both microphones in identical sound fields and record any frequency-dependent phase and amplitude differences. This calibration data was then used by the computer to condition the data prior to the calculation of reactive impedance, phase angle and complex reflection coefficient. In this manner, the effect of differences between the two microphone channels on the data was minimized. Additionally, this method also allowed for imbalances in the A/D converter channels of the signal processor.

The identical sound fields were obtained by mounting the two microphones at the same radial position at the sample end of the tube. This was based on the assumption that the sound field is radially symmetric at frequencies below the sloshing mode. This frequency is given by [Ref. 18]

$$f_{c_o} = \alpha_o c/d \qquad (2.41)$$

where "α_o" is the solution to

$$\frac{d J_n(\pi \alpha)}{d\alpha} = 0 \qquad (2.42)$$

and "d" is the diameter of the tube. The sloshing mode corresponds to "α_o" which is equal to .5861. This results in a cut-off frequency of 2650 Hz. The calibration program used is given in Appendix A.

b. Validation of Tube Performance

After calibration of the microphone channels, the microphones were placed in the normal positions in the wall of the tube and the proper operation of the system was

36

verified. A 4.03 inch long piece of PVC pipe with the same
diameter, provided with a rigid reflective end, was used as
a sample impedance. The expected results were a reflection
coefficient of 1 and a known phase change equal to

$$\Delta\phi = \frac{4\pi L}{\lambda} = \frac{4\pi L f}{c} \qquad (2.43)$$

The results are shown in Figures 2.8 and 2.9 Figure 2.8
shows that the reflection coefficient is approximately 1 for
frequencies below 2.5 kHz. except at 1.5 kHz., were the
phase goes through 0 degrees yielding an indeterminancy
which is discussed in section e. which follows. Above 2.5
kHz. non-plane wave modes degrade the results. The measured
slope of the phase shift versus frequency shown in Figure X
is -53 degrees $\pm$ 1 degree. Using equation (2.41), this slope
produces a sound speed of 356 $\pm$ 1.34 m/sec, which is consis-
tant but significantly higher than the average of the four
values obtained by the SWT technique listed in Tables
II,VII-IX (c = 345.12 $\pm$ .38 m/sec).

    c. Data Collection

        Each of the three Helmholtz resonators was
placed at the sample end and the data collected. The data
was tabulated in Tables X-XII. The collection and recording
of the data was done completely by the computer and the
program is given in Appendix B.

    d. Data Reduction

        After the raw data was collected the first step
was to determine the resonant frequency of the Helmholtz
resonator. The data collected allows this to be done in two
different ways. Both were used. First, the specific reactive
impedance "$X_s / \rho c$" was plotted versus the frequency and a

TABLE X

Dual-Microphone Measured Data - Resonator #1 Run 1

$$f_o = 587.3 \pm 2.2 \text{ Hz.}$$

Freq.	$X_s \angle \rho c$	Phase Angle	360 + Phase Ang.
Hz.	Pa-s/m	deg.	deg.
250	-5.87	0	360
350	-2.83	- 23.9	336.1
400	-1.91	- 41.7	318.3
450	-1.23	- 65.6	294.4
500	-.671*	-105.2	254.8
550	-.256*	-147.6	212.4
600	.114*	166.2	
650	.395*	135.6	
700	.676	110.7	
750	.919	93.9	
1000	1.86	55.2	
1250	2.66	43.2	
1500	3.03	36.5	

Run 2

$$f_o = 590.6 \pm .2 \text{ Hz.}$$

Freq.	$X_s \angle \rho c$	Phase Angle	360 + Phase Ang.
Hz.	Pa-s/m	deg.	deg.
250	2.13	19.2	379.2
300	-1.58	- 8.4	351.6
350	-2.14	- 27.4	332.6
400	-1.64	- 52.2	307.8
450	-1.07	- 78.6	281.4
500	-.591	-113.5	246.5
550	-.224	-152.6	207.4
600	.076	170.8	
650	.350	140.3	
700	.629	114.6	
750	.850	96.0	
800	1.19	79.9	
900	1.52	66.5	
1000	2.22	47.8	
1250	2.96	37.1	
1500	3.17	34.9	

linear regression was used done using the two points on either side of the origin (4 points total) where the reactive impedance was equal to zero. This gives the resonant frequency since the reactive impedance of a resonator equals zero at resonance. The graphs and resonant frequencies for each resonator are shown in Figures 2.10-2.14

The second method for determining the resonant frequency involved the use of the phase angle between the incident and reflected waves. When the phase angle was plotted versus frequency (Figures 2.15-2.19) resonance was obtained from the graph at the point where the phase angle was 180 degrees. Again a linear regression was used with the 2 points on either side of the 180 degree phase angle. Figures 2.15-2.19 also show the frequency determined. The resonant frequency used in subsequent calculations was the average of the two frequencies determined from the two methods. The reproducibility of the results can be estimated from the ratio of the standard deviation to the average for the four (two) separate measurements of the resonant frequencies for resonators 1 and 2, which were 0.5% and 2.0%, respectively.

Once the resonant frequency was determined, it was used along with equation (2.13)

$$X_m^! = f - f_o^2/f \tag{2.13}$$

to obtain "$X_m^!$". Using this along with the reactive impedance ratio "$X_s/\rho c$", the experimental value for the ratio

$$K_{exp} = \frac{X_s/\rho c}{X_m^!} \tag{2.42}$$

39

TABLE XI

Dual-Microphone Measured Data - Resonator #2 Run 1

$f_o = 435.8 \pm 3.8$ Hz.

Freq. Hz.	$X_s \angle \rho c$ Pa-s/m	Phase Angle deg.	360 + Phase Ang. deg.
200	.215	7.5	367.5
250	-4.24	- 1.6	358.4
300	-.151	- 8.3	351.7
350	-.436	- 47.3	312.7
400	-.206	-121.7	238.3
450	.100	164.6	
500	.386	133.0	
550	.667	109.7	
600	.893	94.8	
650	1.07	85.0	
700	1.27	76.0	
750	1.40	70.4	
800	1.60	63.8	
900	1.84	56.7	
1000	2.12	50.1	
1250	2.57	42.2	
1500	2.83	38.1	

Run 2 $f_o = 421.7 \pm .3$ Hz.

Freq. Hz.	$X_s \angle \rho c$ Pa-s/m	Phase Angle deg.	360 + Phase Ang. deg.
200	.163	- 1.6	361.6
250	-2.03	- 41.7	318.3
300	-.987	- 87.4	272.6
350	-.434	-132.5	227.5
400	-.082	-170.5	189.5
450	.171	160.0	
500	.412	134.4	
550	.593	116.9	
600	.813	100.7	
650	.993	89.8	
700	1.27	75.7	
750	1.50	67.1	
800	1.78	58.4	
900	1.91	54.8	
1000	2.65	41.2	
1250	3.35	33.2	
1500	3.38	33.0	

40

$f_o = 947.1 \pm 1.0$ Hz.

Freq. Hz.	$X_s \angle \rho c$ Pa-s/m	Phase Angle deg.	360 + Phase Ang. deg.
400	.719	22.1	382.1
450	.174	5.6	365.6
500	-.039	- .9	359.1
550	-.597	- 15.4	344.6
600	-1.01	- 25.4	334.6
650	-1.06	- 34.6	325.4
700	-.921	- 56.4	303.6
750	-.834	- 69.4	290.6
800	-.625	- 94.6	265.4
850	-.380	-126.9	233.1
900	-.201	-150.7	209.3
950	.048	173.5	
1000	.196	155.2	
1050	.385	135.5	
1100	.571	118.1	
1200	1.05	86.5	
1300	1.34	73.0	
1400	1.57	64.7	
1500	1.69	61.2	

was calculated for comparison with the theoretical value obtained from equation (2.23)

$$K_{th} = \frac{-2\pi L' A_1}{c\, A_2}$$ (2.23)

Tables XIII-XV show the results for "K_{exp}" for each of the resonators tested.

e. Error Analysis

The Chung-Blaser dual-microphone technique had some inherent errors built into it by virtue of the equipment construction and mathematical techniques. First, the

41

TABLE XIII

Dual-Microphone Reduced Data - Resonator #1 Run 1

Frequency Hz.	X'_m s^{-1}	K_{exp} x 10^{-3}
250	-1142	5.14*
350	- 644.2	4.39
400	- 470.0	4.06
450	- 323.3	3.80
500	- 196.0	3.42
550	- 82.7	3.10*
600	20.0	5.69*
650	114.6	3.45
700	202.9	3.33
750	286.0	3.21
1000	652.0	2.85
1250	971.6	2.74
1500	1268	2.39
	average	3.52
	deviation	.79
	per cent	22.4

Run 2

Frequency Hz.	X'_m s^{-1}	K_{exp} x 10^{-3}
250	-1146	1.86*
300	- 863.1	1.83*
350	- 646.9	3.31
400	- 472.3	3.47
450	- 325.4	3.29
500	- 197.9	2.97
550	- 84.4	2.65*
600	18.5	4.12*
650	113.2	3.09
700	201.5	3.12
750	284.8	3.13
800	363.8	3.27
900	512.3	2.97
1000	651.1	3.41
1200	909.2	3.26
1400	1151	2.75
	average	3.17
	deviation	.21
	per cent	6.62

*Values not used for the calculation of the average.

TABLE XIV

Dual-Microphone Reduced Data - Resonator #2 Run 1

Frequency Hz.	X'_m s^{-1}	K_{exp} x 10^{-3}
200	- 749.6	.29*
250	- 509.7	8.32*
300	- 333.1	.45*
350	- 192.6	2.26
400	- 74.8	2.75
450	28.0	3.58*
500	120.2	3.21
550	204.7	3.26
600	283.5	3.15
650	357.8	2.99
700	428.7	2.96
750	496.8	2.82
800	562.6	2.84
900	689.0	2.67
1000	810.1	2.62
1200	1042	2.47
1400	1264	2.24
	average	2.79
	deviation	.33
	per cent	11.8

Run 2

Frequency Hz.	X'_m s^{-1}	K_{exp} x 10^{-3}
200	- 689.6	.24*
250	- 461.7	4.40*
300	- 293.1	3.37
350	- 158.3	2.74
400	- 44.8	1.83*
450	54.6	3.13
500	144.2	2.86
550	226.5	2.62
600	303.5	2.69
650	376.3	2.64
700	445.8	2.85
750	512.8	2.93
800	577.6	3.08
900	702.3	2.72
1000	822.1	3.22
1200	1052	3.18
1400	1273	2.66
	average	2.91
	deviation	.25
	per cent	8.59

*Values not used in the calculation of the average.

TABLE XV

Dual-Microphone Reduced Data - Resonator #3

Frequency Hz.	X'_a s^{-1}	K_{exp} x 10^{-3}
400	-1844	.39*
450	-1545	.11*
500	-1295	.03*
550	-1082	.06*
600	- 895.9	1.13
650	- 730.9	1.45
700	- 582.2	1.58
750	- 446.8	1.87
800	- 322.0	1.94
850	- 206.0	1.84
900	- 97.3	2.07
950	5.2	9.24*
1000	102.4	1.91
1050	195.2	1.97
1100	284.0	2.01
1200	452.0	2.32
1300	609.6	2.20
1400	758.9	2.07
1500	901.6	1.87

average	1.91
deviation	.23
per cent	12.0

* Values not used in the calculation of the average.

construction of the tube limits the range of frequencies over which good data could be obtained. The diameter of the tube determined the upper limit of measurable frequency. Since the tube was valid only for a plane wave, the frequencies measured had to be below the cutoff frequency for the tube. For the tube used in this study the cutoff frequency was approximately 2600 Hz. The construction of the tube also limits the effectiveness of measurements at the lower frequencies. The critical parameter in this case is the spacing between the microphones. For a given separation as

the wavelength gets longer (frequency lower), the differences in the phase and amplitudes at the two microphone locations became small and the noise dominated. The low frequency limit for the tube was about 200 Hz.

Finally, the mathematical technique resulted in an indeterminacy in the reflection coefficient. This occurred when the phase angle was equal to zero. When this occurred equation (2.35) reduced to

$$R = 0/0$$

which is indeterminant. The result was that data obtained for the frequencies about 50 Hz on either side of the point where the phase angle equalled zero was greatly in error.

D. COMPARISON OF THE TWO TECHNIQUES

The two techniques were consistant with each other and with the expected theoretical values. First, the techniques will be locked at for comparison with the the theoretical results and then for comparison with each other.

1. Standing Wave Tube Technique

Figures 2.20-2.22 show the comparison of the experimental and theoretical values for "$X_s/\rho c$". The theoretical values were obtained using "K_{th}" (eqn. 2.23) and the calculated values for "X_m'" (Tables VII-IX). These were tabulated in Tables VII-IX As can be seen in Figures 2.20-2.22 the values compare favorably with a divergence noted at the higher frequencies away from resonance. This divergence was explained in the error analysis in section B.3.c.

Table XVI shows the resonant frequency and both constants for each resonator, along with the resonant frequency determined by the independent method discussed in section B.3.c. As can be seen, "K_{exp}" and "K_{th}" were within

45

the calculated error for each. The average per cent error
between the two values for "K " was found to be 4.13% for
the standing wave tube technique. The average per cent error
for the resonant frequency was found to be -2.23%.

2. Chung-Blaser Dual-Microphone Technique

Figures 2.23-2.27 show the comparison of the experi-
mental and theoretical values for "$X_s/\rho c$". The theoretical
values were obtained in the same manner as in the SWT tech-
nique. The graphs show a good agreement except at the lower
and higher frequencies away from resonance for reasons
previously noted in section C.3.e.

Table XVI shows the resonance frequency and both
values obtained for the dual-microphone technique.   The
values determined for "K_{exp}" and "K_{th}" do not in all cases
overlap within the areas of uncertainty as was the case with
the SWT technique. As a result, the average per cent error
(($K_{exp} - K_{th})/K_{th}$) x 100 was found to be 18.4%. The average per
cent error between the independently measured resonant
frequency and that measured by the dual-microphone method
was found to be +11.4%.

3. Standing Wave Tube vs. Dual-Microphone

The greatest discrepancy between the two methods was
the measured resonant frequencies. The resonant frequency
measured by the dual-microphone technique was always higher
than the resonant frequencies measured by the other two
methods. The average error of +11.4% was significantly
larger than the error for the standing wave tube method of
-2.23%. Additionally, the determination of the constants
for the dual-microphone method produced larger discrepancies
between the theoretical and experimental values. Finally,
the calculated sound speed for the dual-microphone method
was 3.2% higher than the SWT method which was in good

46

TABLE XVI
Comparison of Results

	Freq. Hz.	K_{th} sec. $\times 10^{-3}$	K_{exp} sec. $\times 10^{-3}$	$\dfrac{K_{exp} - K_{th}}{K_{th}} \times 100$ %
RES #1				
549.5 ± 1.5 Hz.				
SWT	542.7	7.35 ± .18	7.57 ± .39	+2.99
Dual run 1	589.5	3.67 ± .10	3.52 ± .79	+4.09
Dual run 2	590.5	3.66 ± .10	3.17 ± .21	-13.4
RES #2				
398.5 ± 3.5 Hz.				
SWT	387.4	7.37 ± .15	6.94 ± .41	-5.83
Dual run 1	432.0	3.45 ± .33	2.79 ± .33	-19.1
Dual run 2	422.0	3.68 ± .07	2.91 ± .25	-20.9
RES #3				
795.0 ± 4.0 Hz.				
SWT	773.0	3.61 ± .09	3.74 ± .47	+3.60
Dual run 1	974.4	1.42 ± .04	1.91 ± .23	+34.5

PER CENT ERROR IN RESONANT FREQUENCY

Resonator #1 - 549.5 Hz.

SWT	-	542.7 Hz.	-1.24%
Dual	-	590.3 Hz.	+7.42%

Resonator #2 - 398.5 Hz.

SWT	-	387.4 Hz.	-2.79%
Dual	-	428.8 Hz.	+7.60%

Resonator #3 - 795.0 Hz.

SWT	-	773.0 Hz.	-2.77%
Dual	-	974.4 Hz.	+22.6%

agreement with the expected sound speed, based on the ambient temperature.
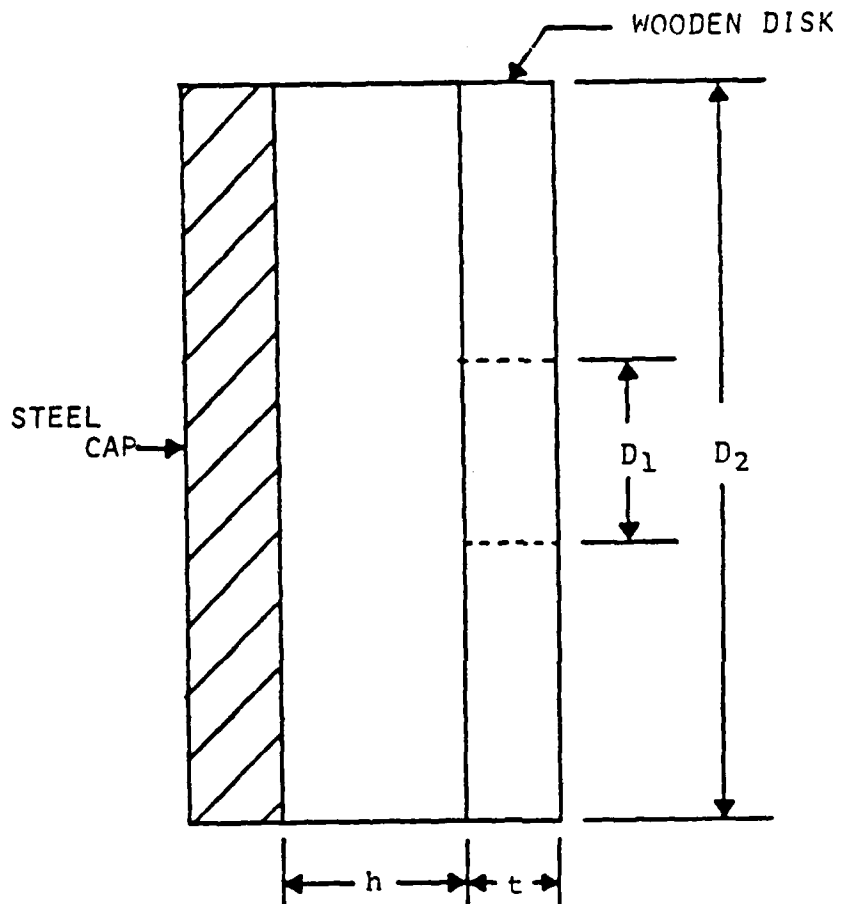
Figure 2.1   Helmholtz Resonator Physical Set-Up.

49
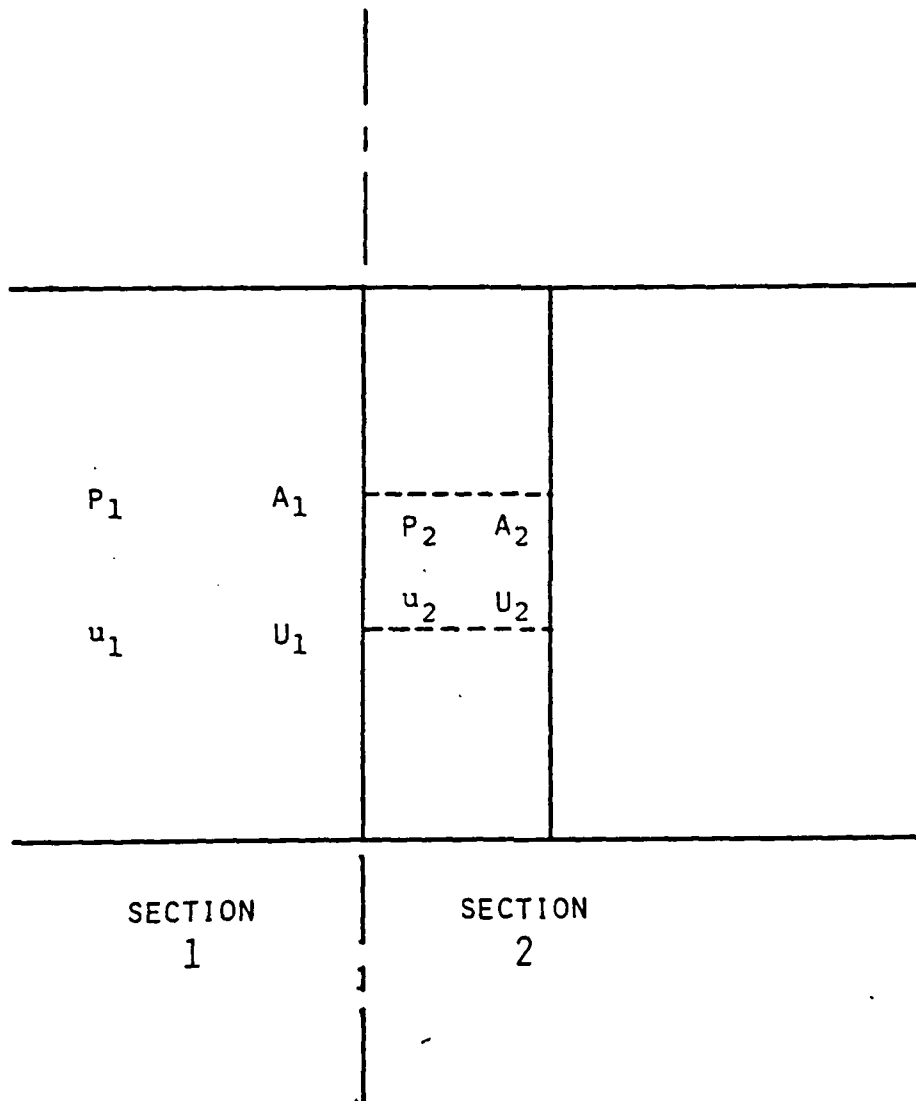
Figure 2.2   Theoretical Helmholtz Resonator Arrangement.
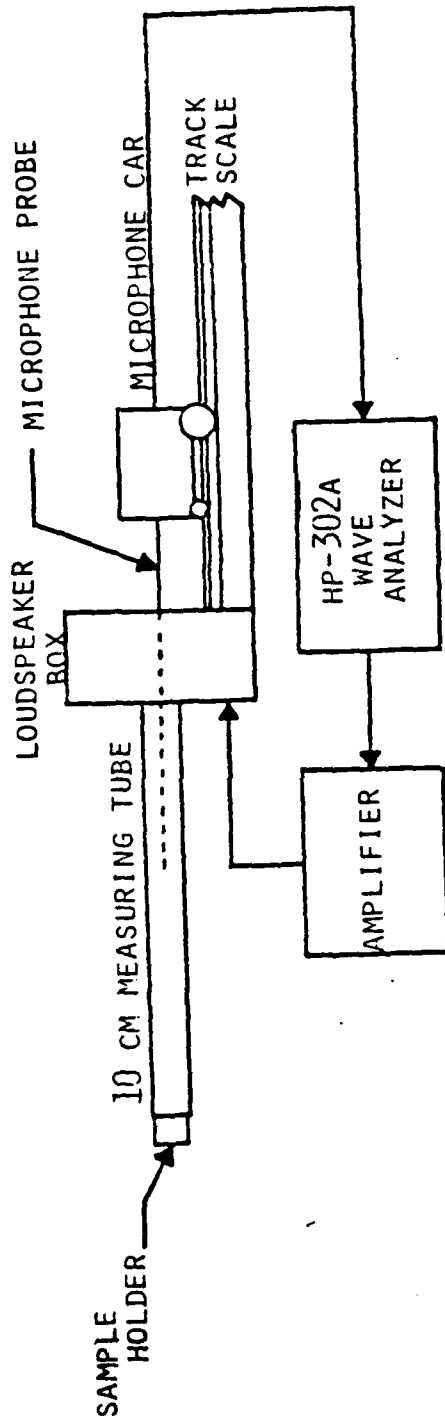
Figure 2.3 Standing Wave Tube Equipment Set-Up.

51
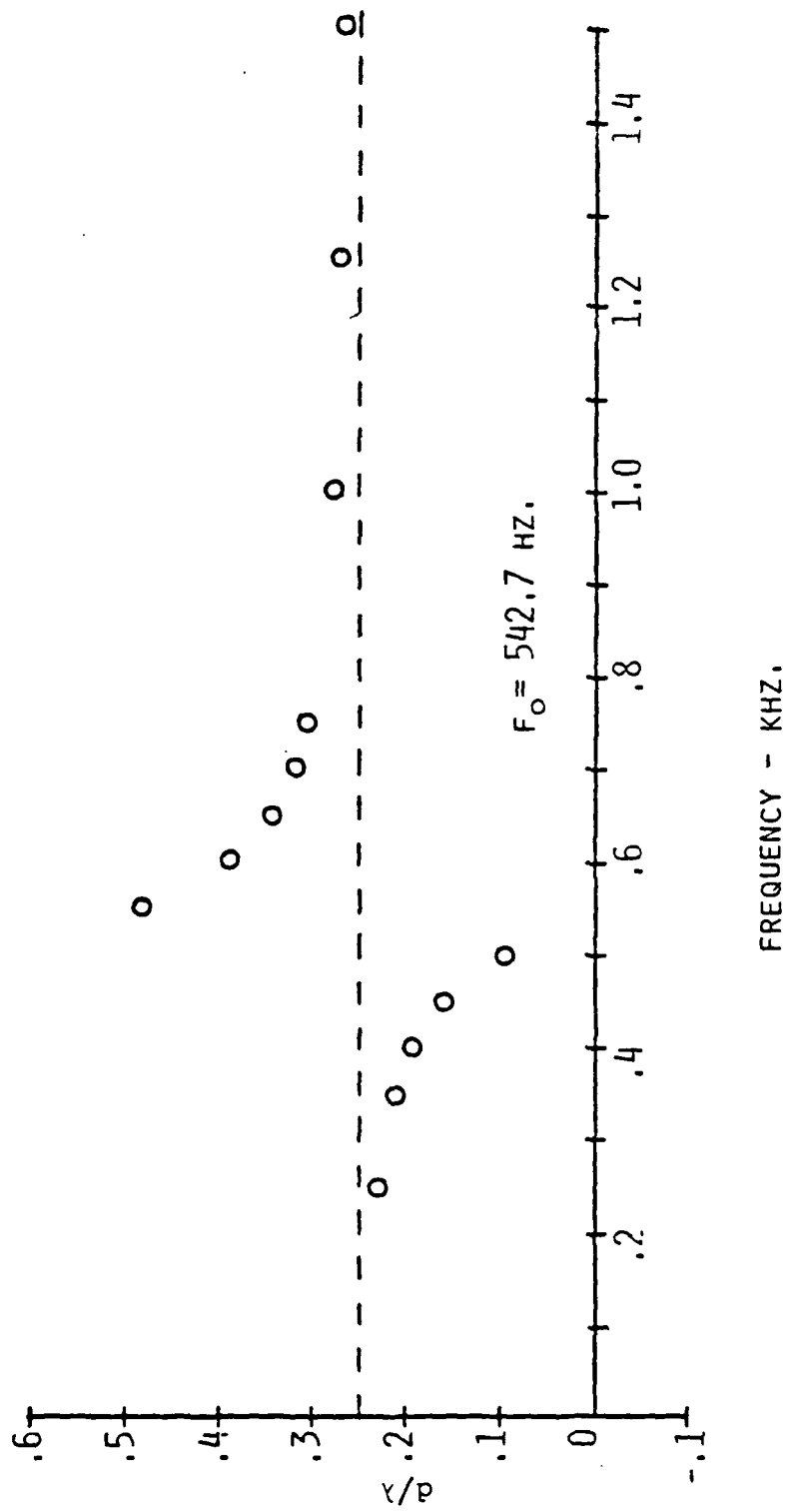
Figure 2.4   Resonator #1 Graph of d/λ vs. Frequency.

FREQUENCY - KHZ.

$F_o = 387.8$ HZ.

d/λ
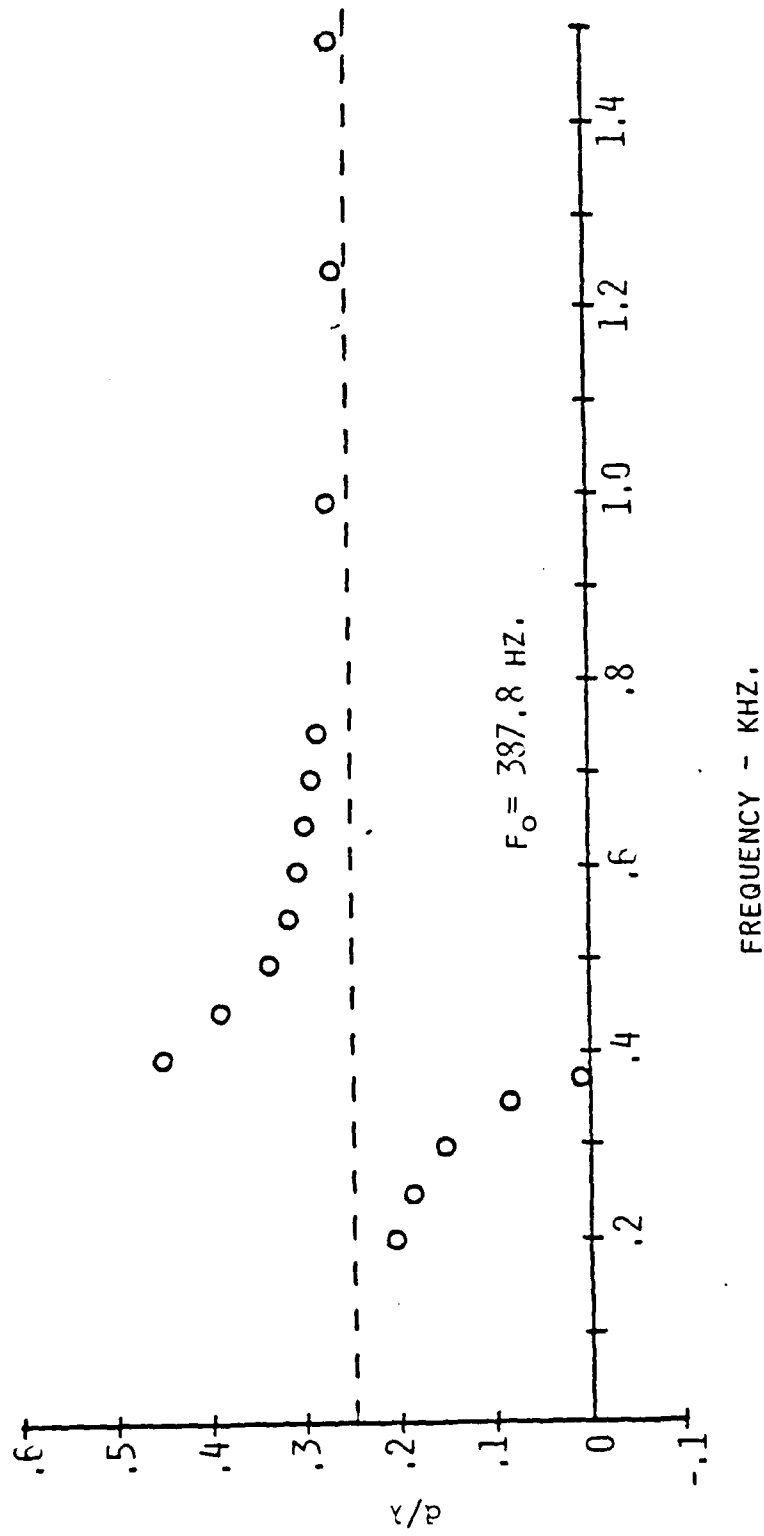
Figure 2.5   Resonator #2 Graph of d/λ vs. Frequency.

53

FREQUENCY - KHZ.

$F_o = 773.0$ HZ.

d/λ
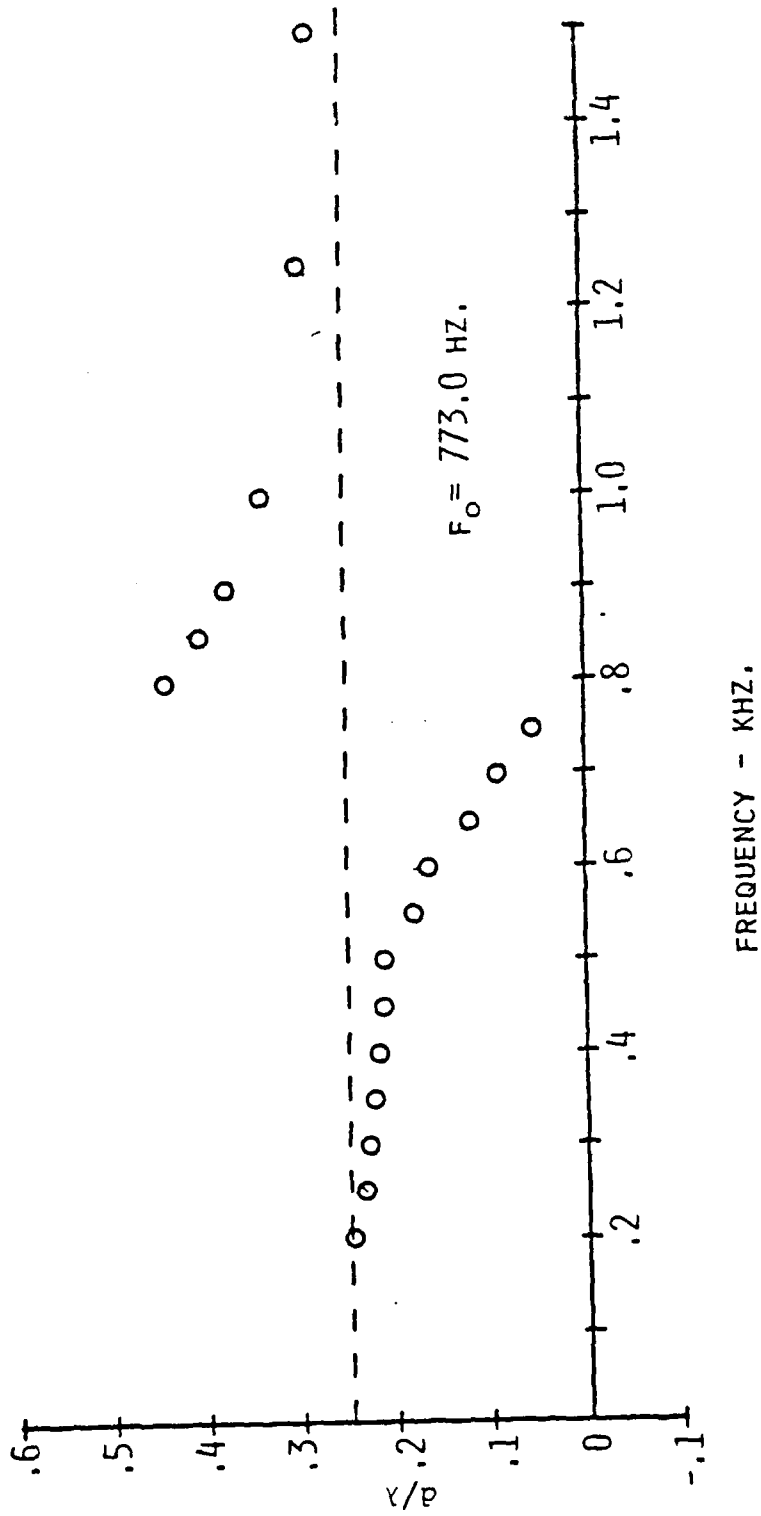
Figure 2.6   Resonator #3 Graph of d/λ vs. Frequency.

54
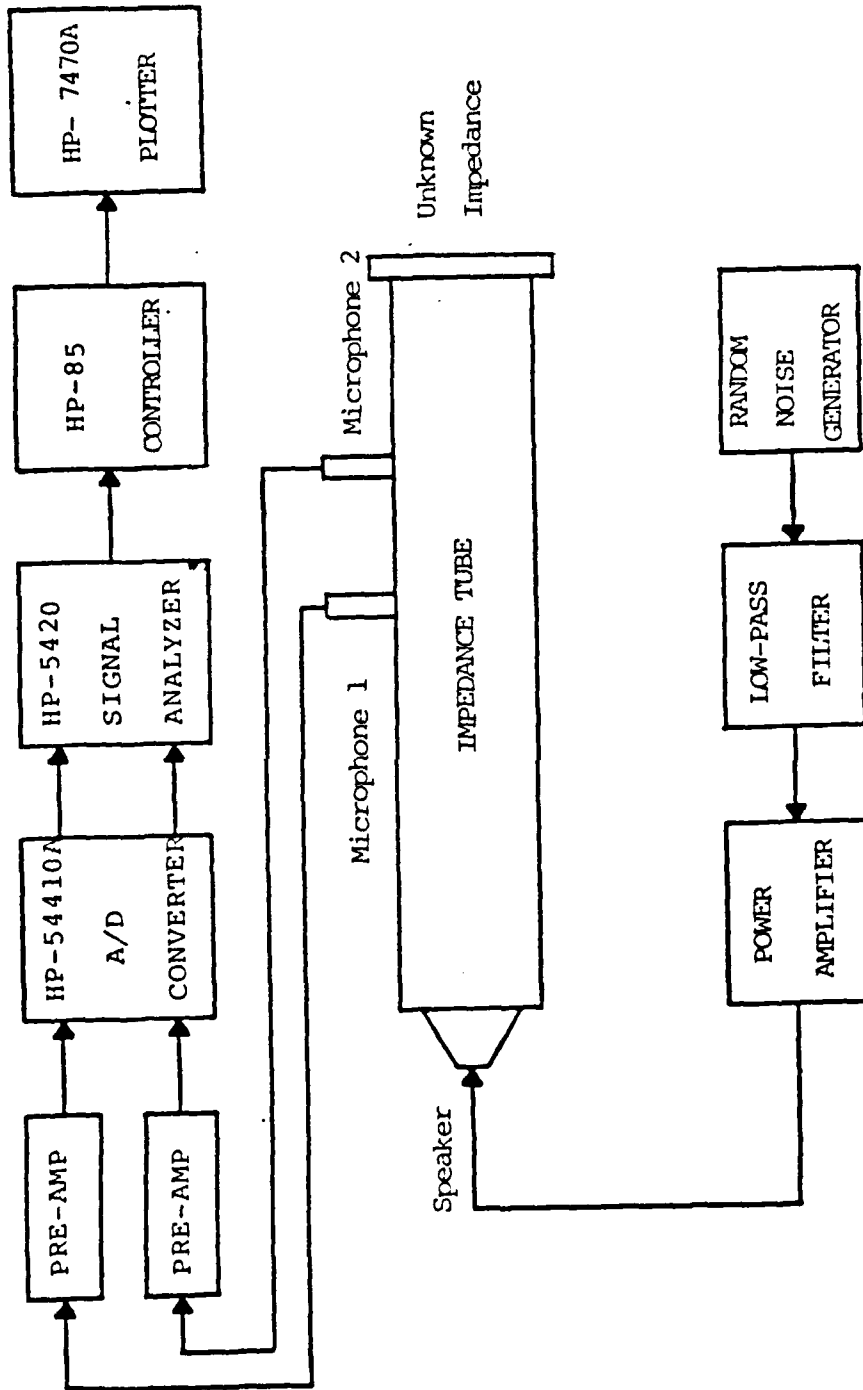
Figure 2.7   Dual-Microphone Technique Equipment Set-Up.

55
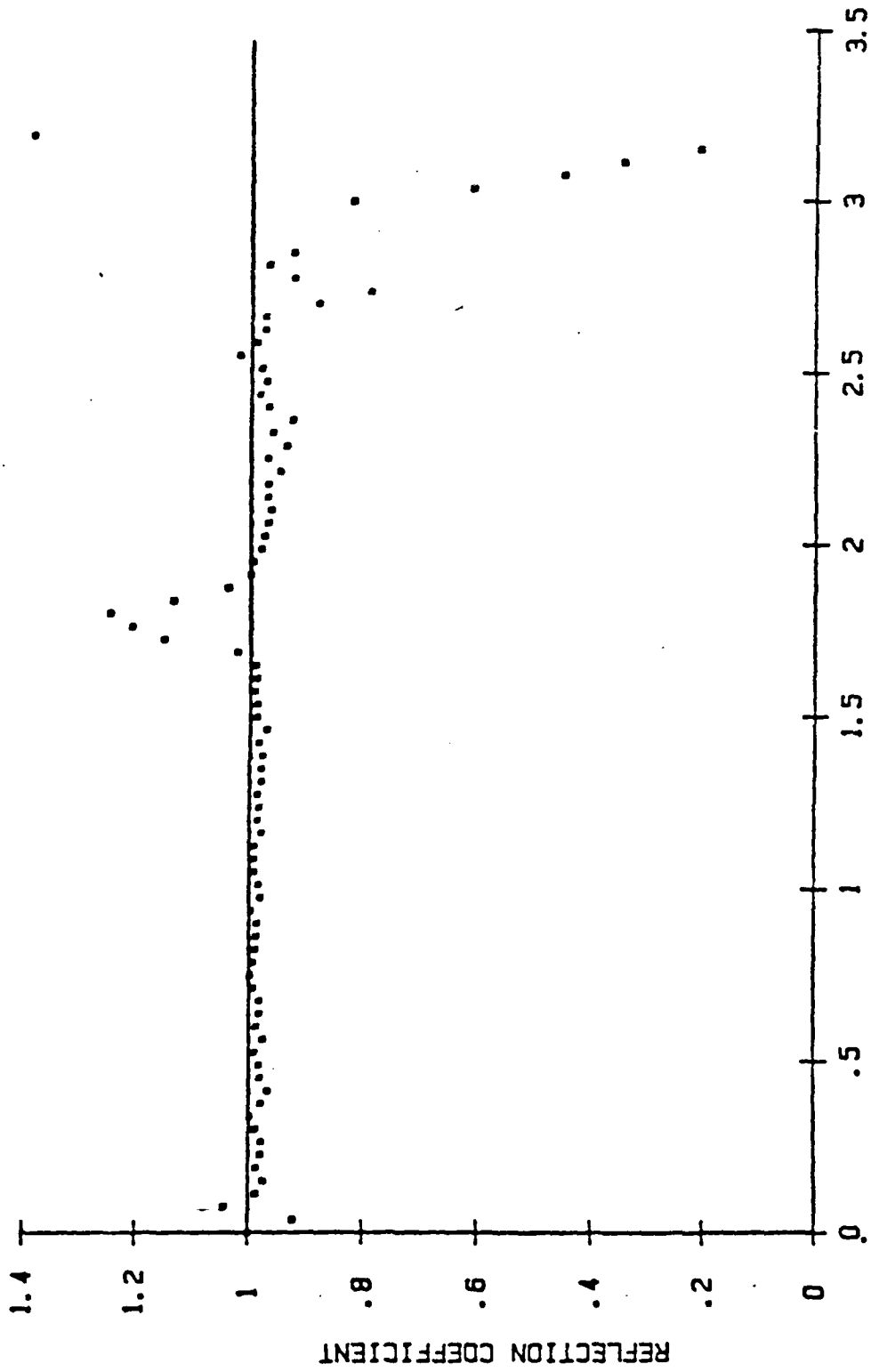
FREQUENCY-KHZ

Figure 2.8   Reflection Coefficient vs. Frequency - Rigid End.

REFLECTION COEFFICIENT
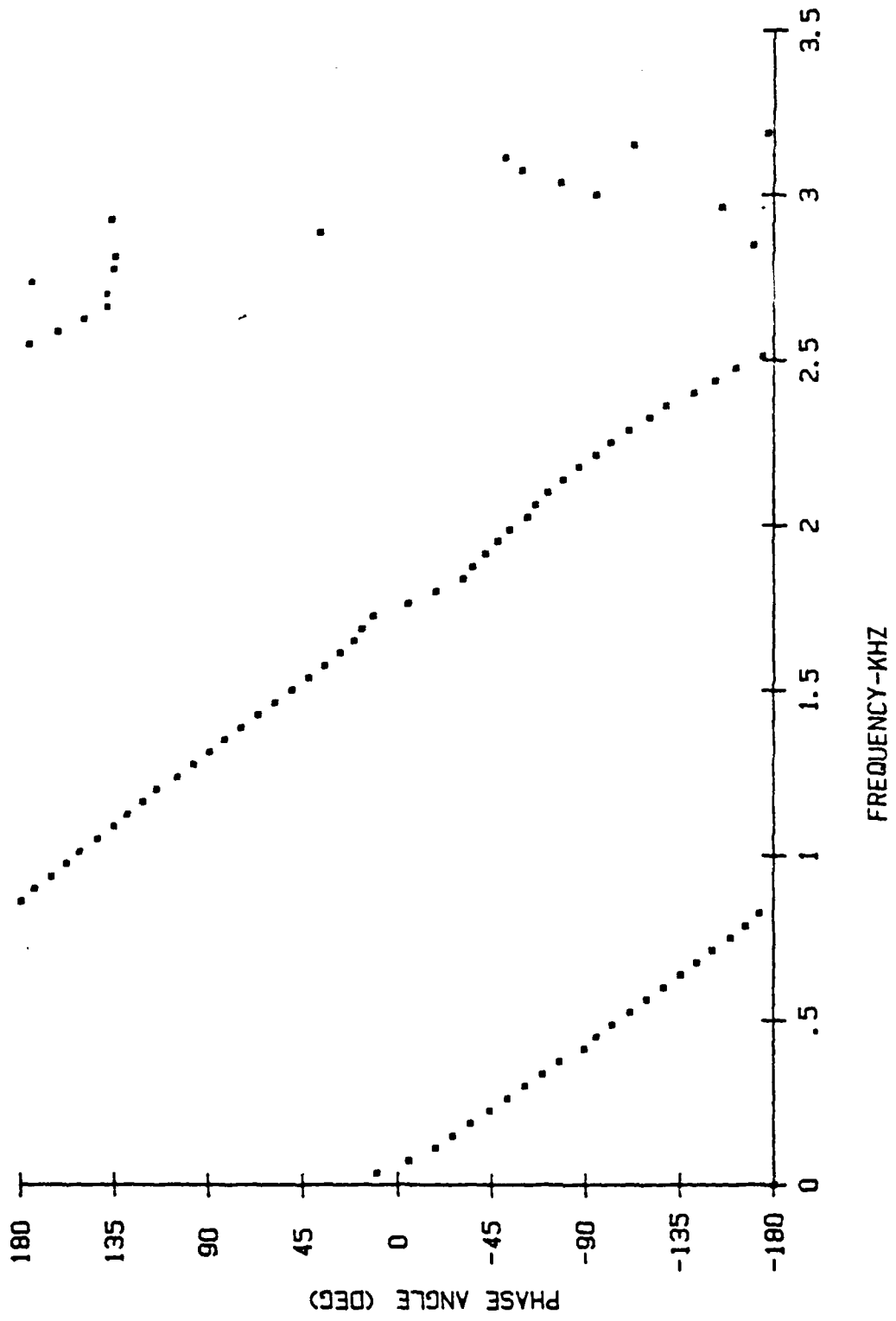
Figure 2.9   Phase Angle vs. Frequency – Rigid End.
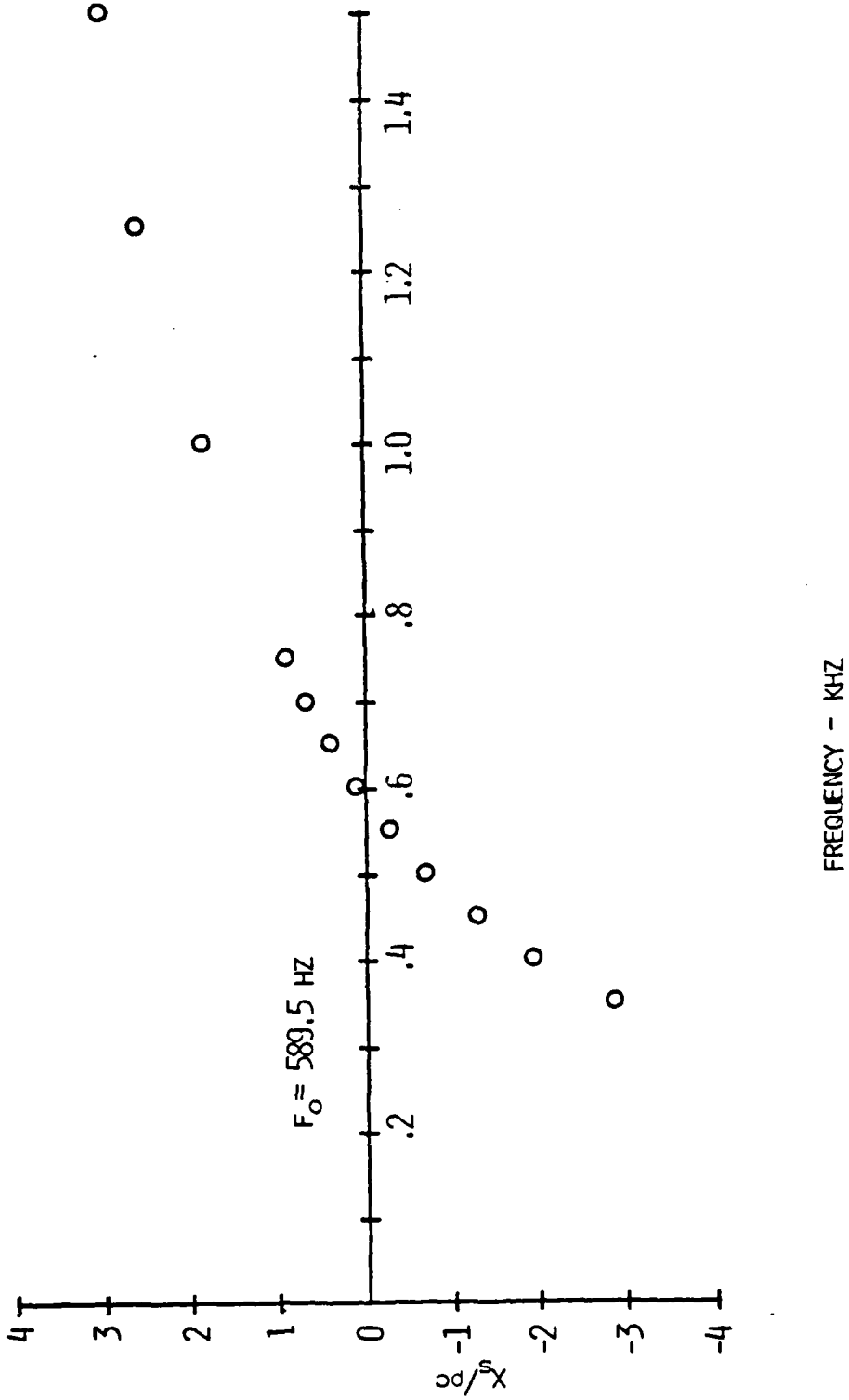
FREQUENCY – KHZ

Figure 2.10   Dual-Microphone "$X_s/\rho c$" vs. Freq. – Resonator #1 Run 1.
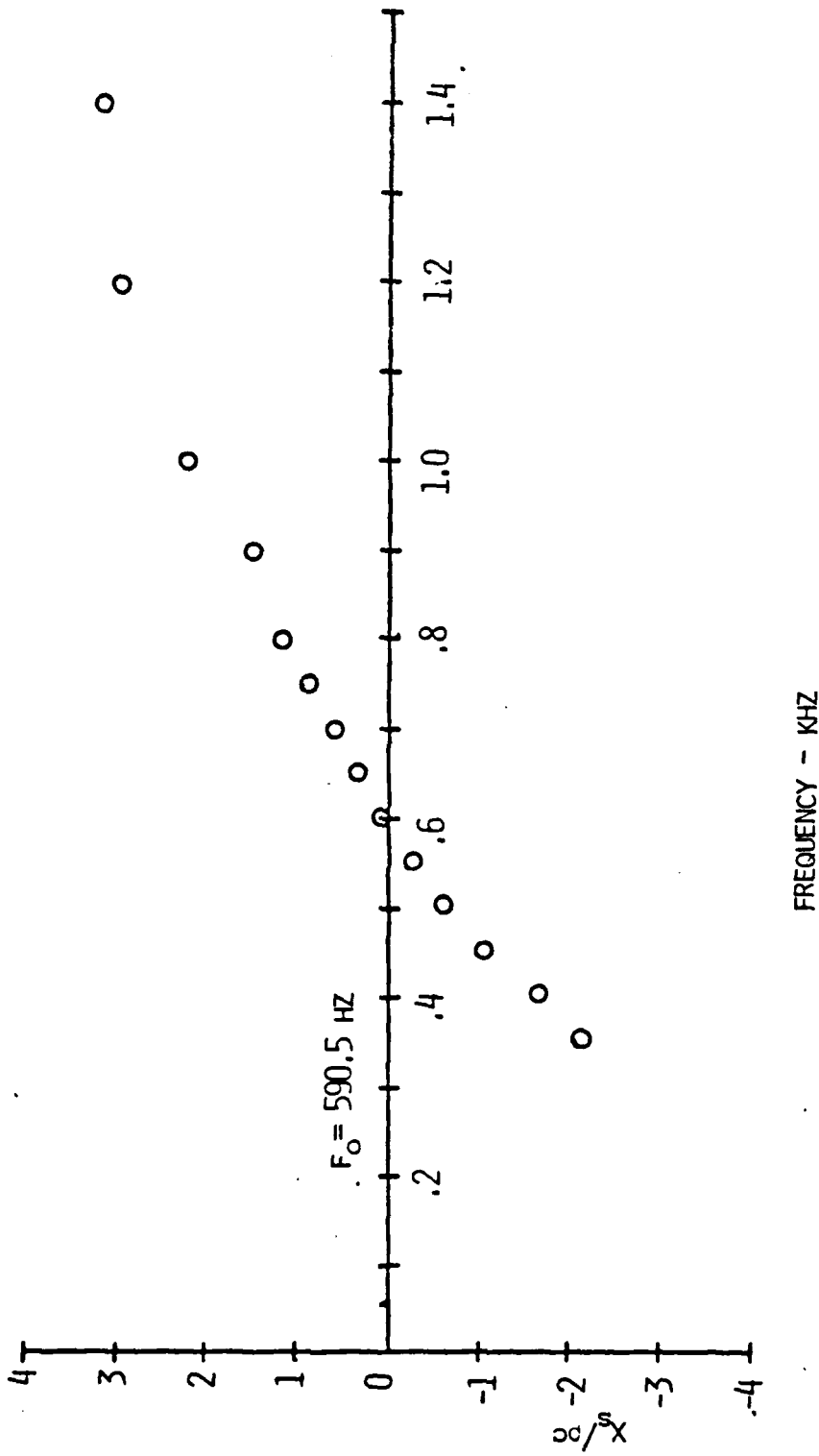
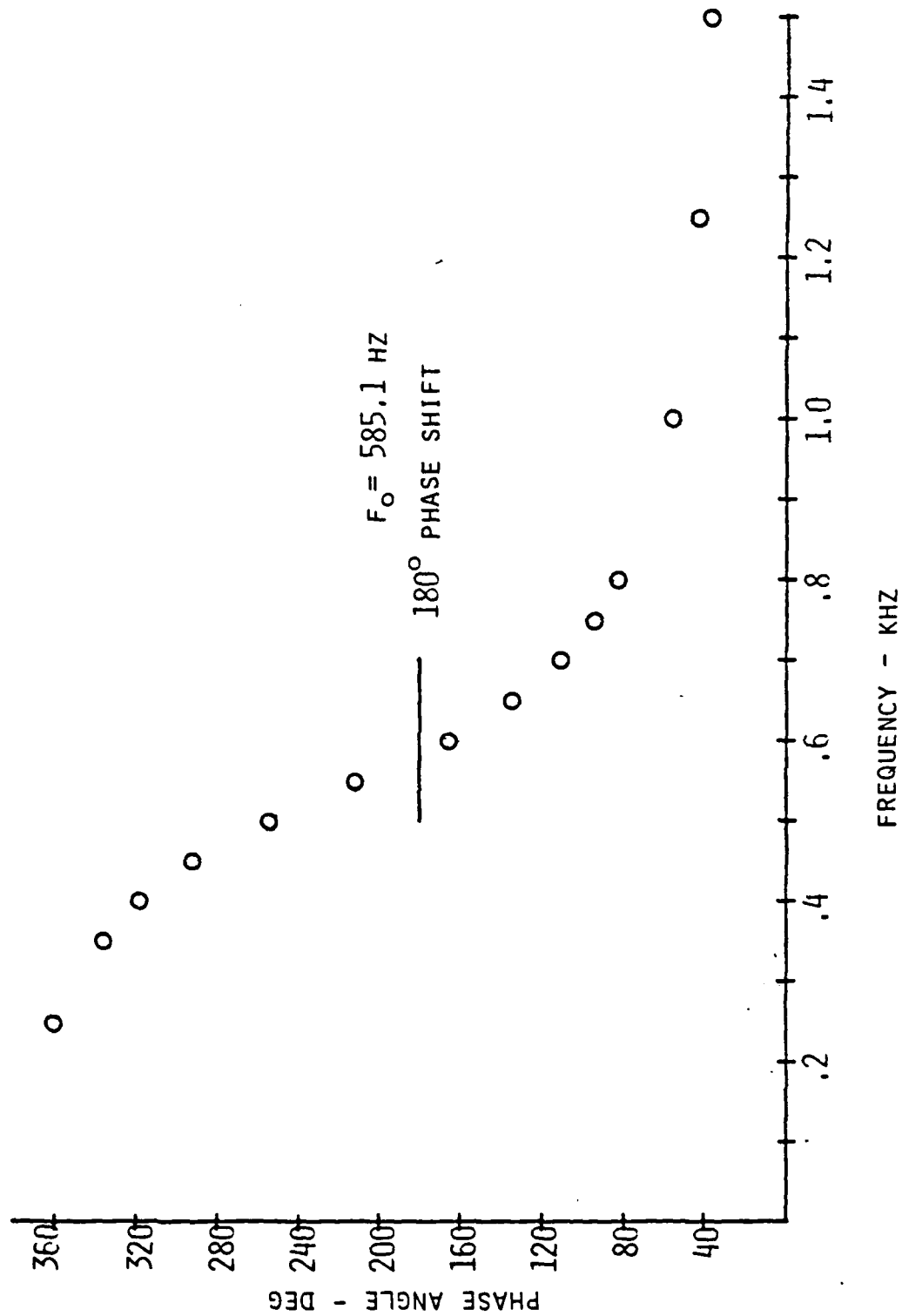Figure 2.11   Dual-Microphone "$X_s/\rho c$" vs. Freq. - Resonator #1 run 2.

FREQUENCY - KHZ

$F_o = 590.5$ HZ

$X_s/\rho c$

FREQUENCY - KHZ

$F_o = 432.0$ HZ

$X_s/\rho c$
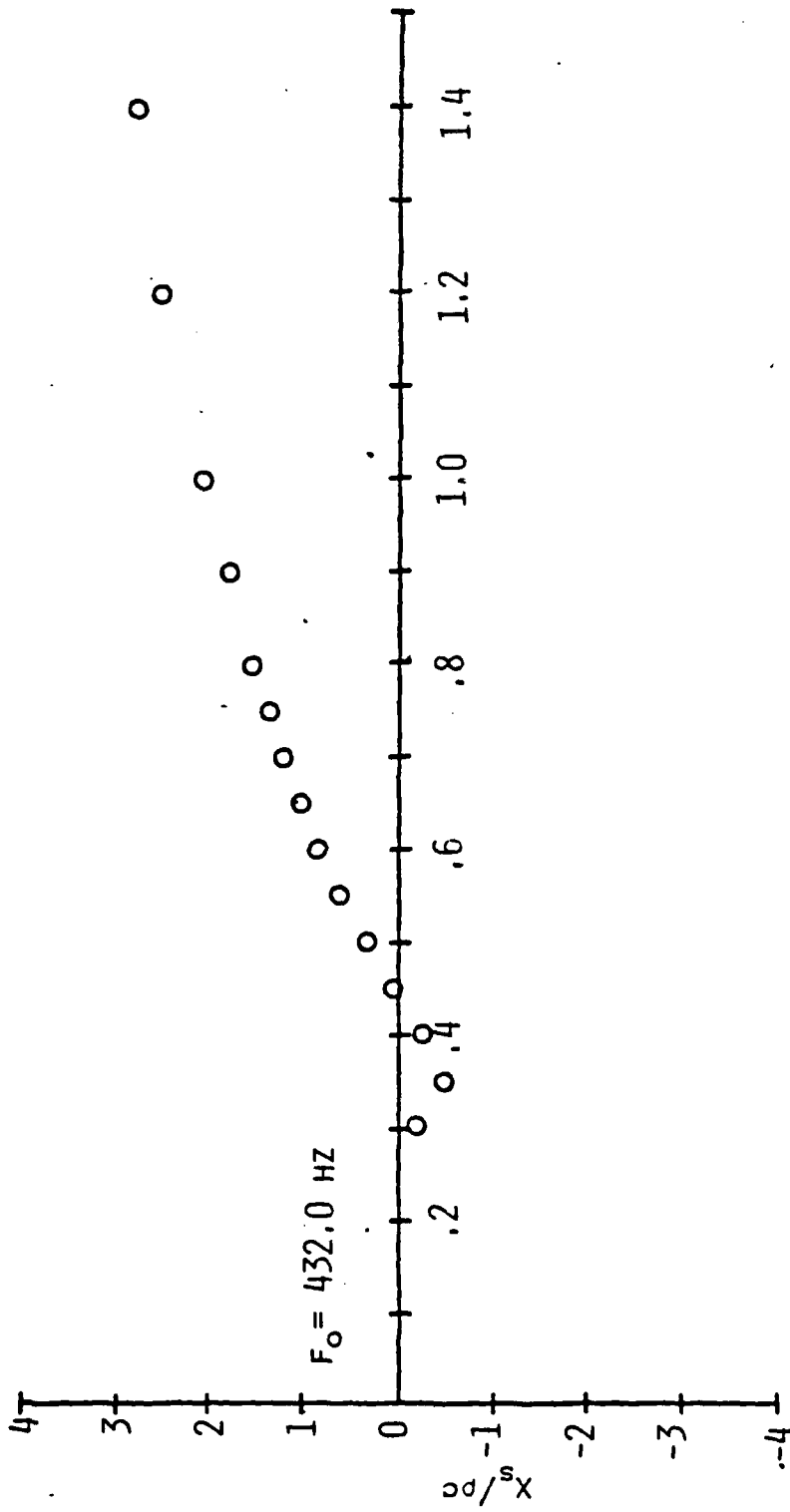
Figure 2.12   Dual-Microphone "$X_s/\rho c$" vs. Freq. - Resonator #2 Run 1.
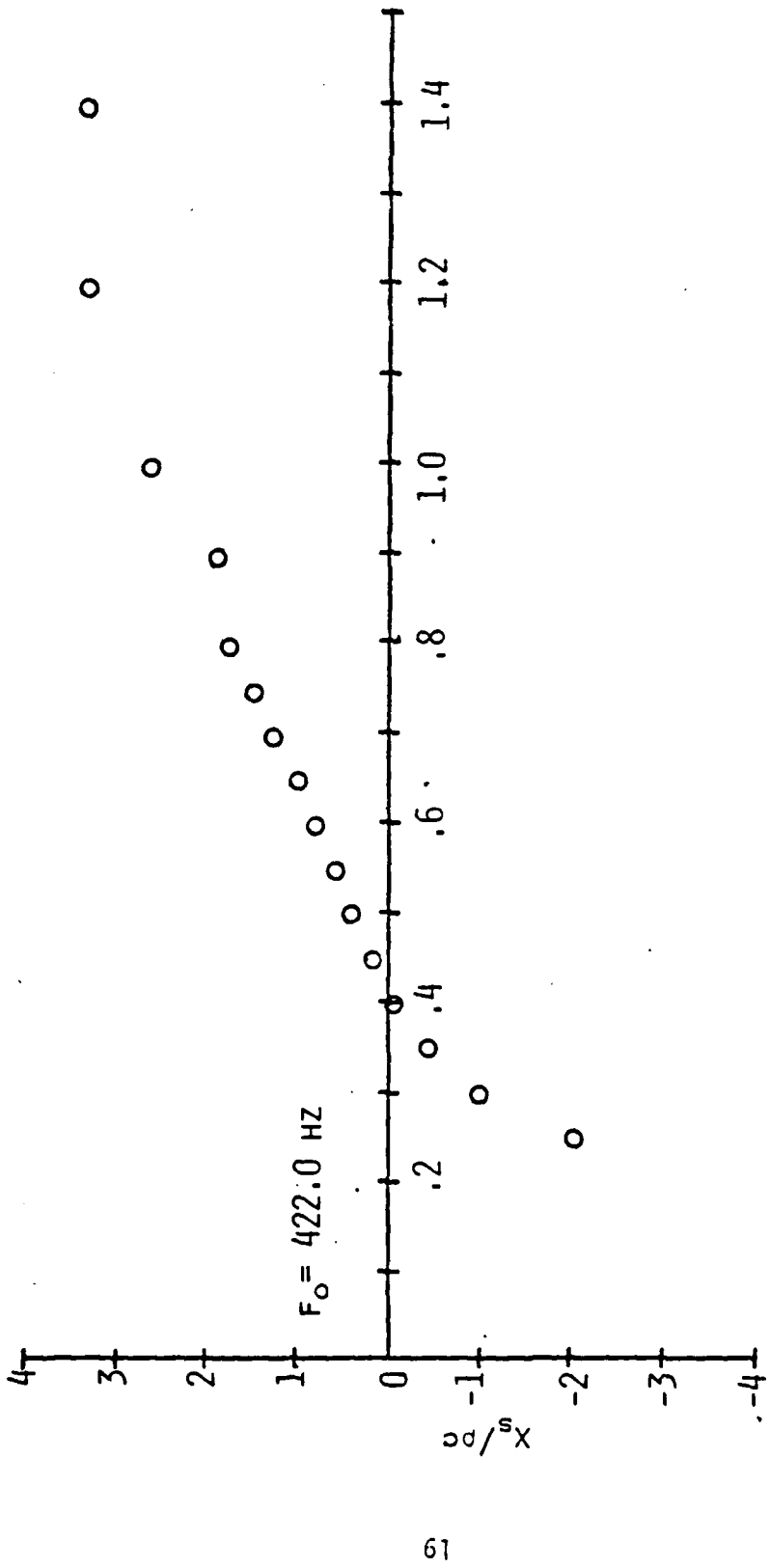
Figure 2.13 Dual-Microphone "$X_s/\rho c$" vs. Freq. - Resonator #2 Run 2.

$F_o = 946.1$ HZ

FREQUENCY - KHZ

1.4 1.2 1.0 .8 .6 .4 .2

$\frac{X_s}{\rho c}$

2 1 0 -1 -2
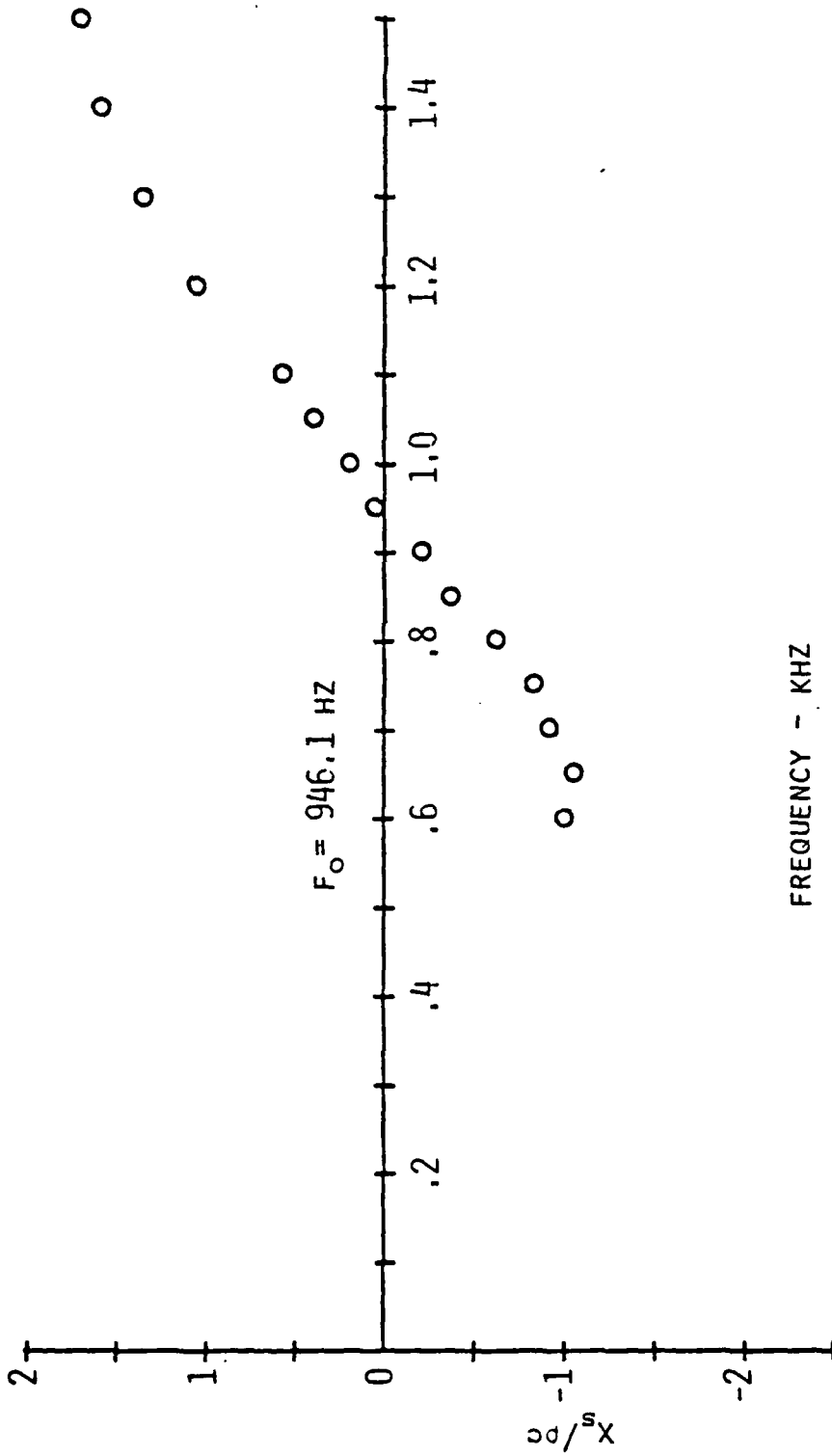
Figure 2.14 Dual-Microphone "$X_s/\rho c$" vs. Freq. - Resonator #3.

62

$F_o = 585.1$ HZ

180° PHASE SHIFT

PHASE ANGLE - DEG

FREQUENCY - KHZ

Figure 2.15   Dual-Microphone Phase Ang. vs. Freq. - Resonator #1 Run1.
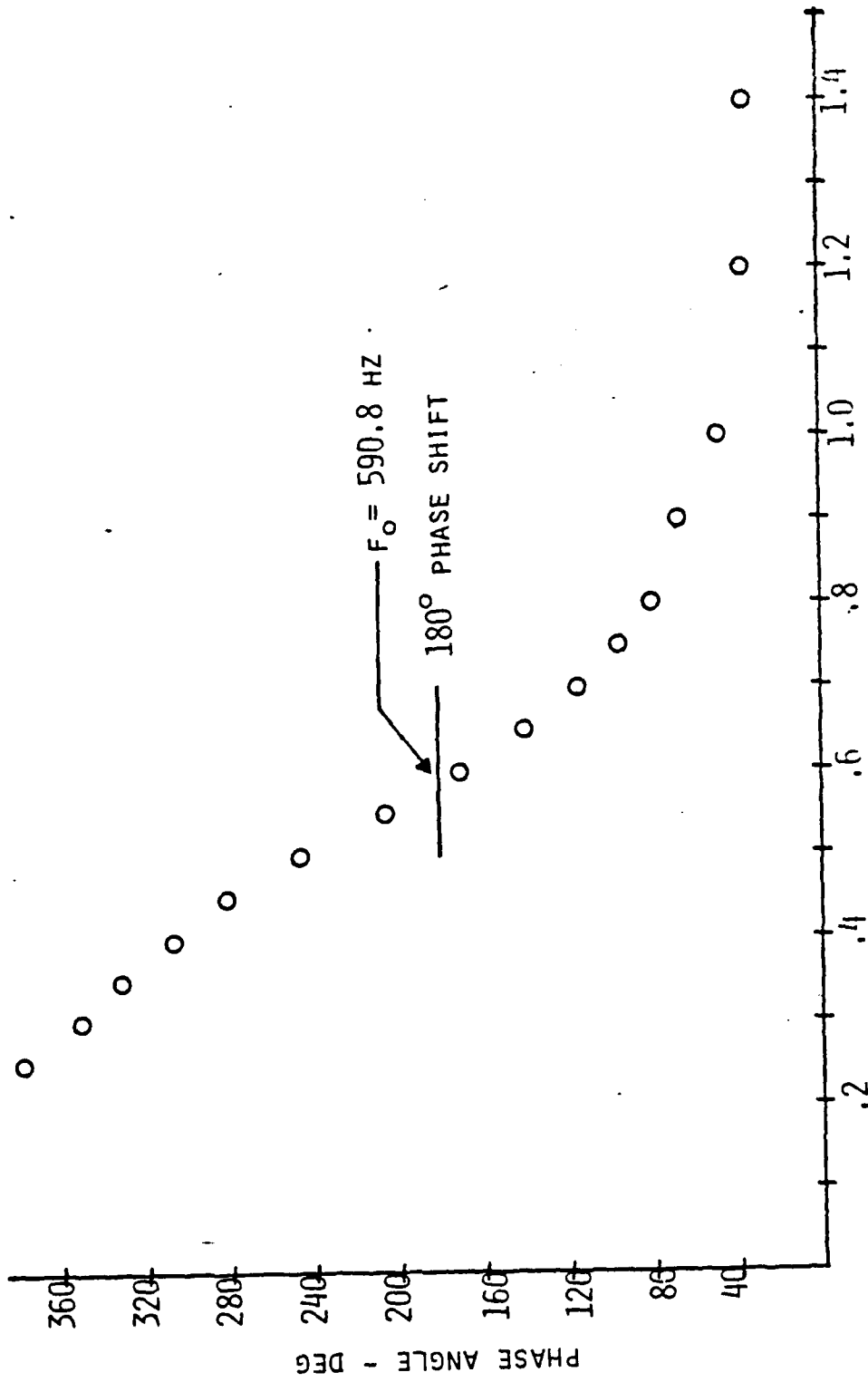
Figure 2.16 Dual-Microphone Phase Ang. vs. Freq. - Resonator #1 Run 2.

64
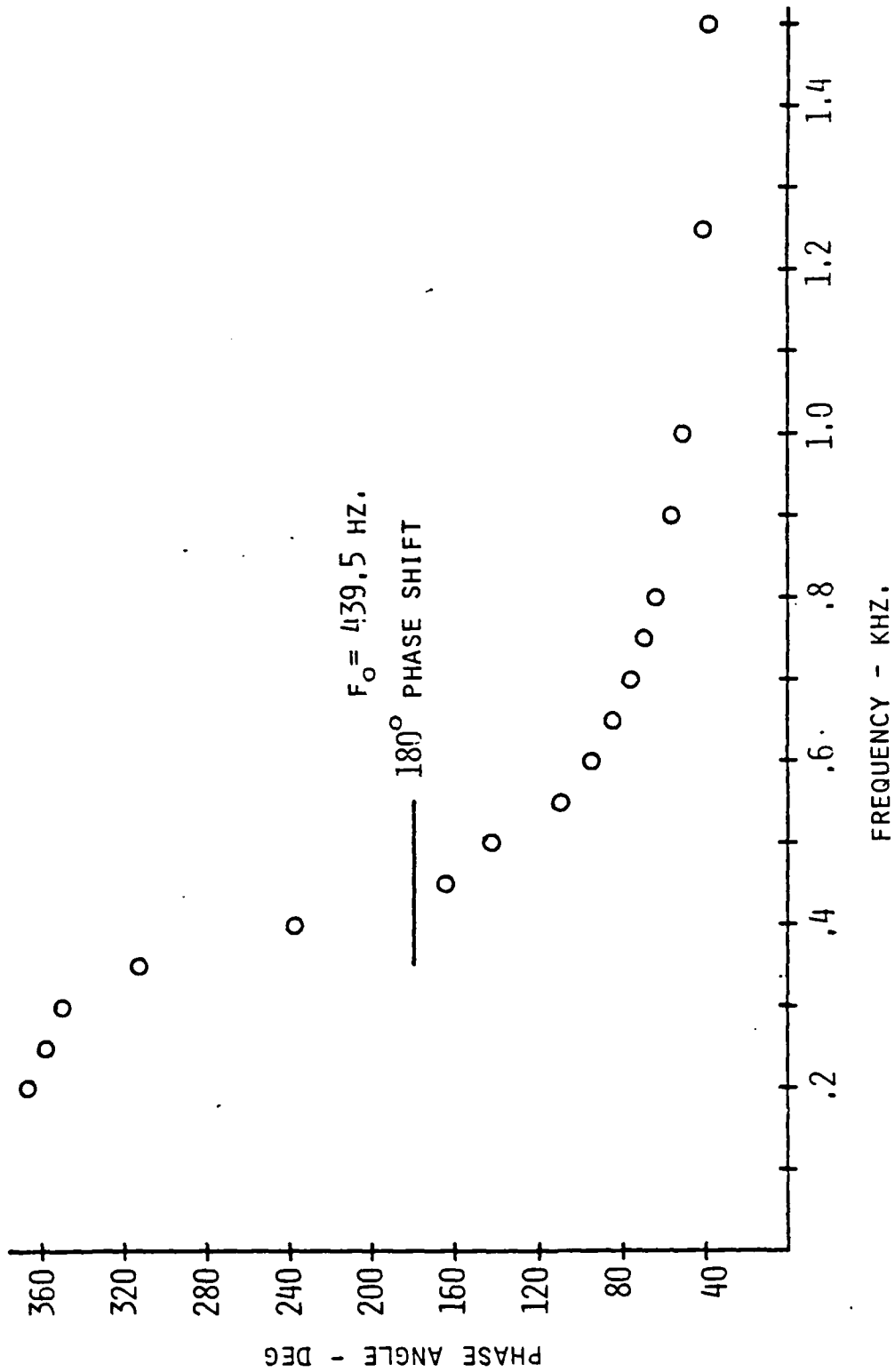
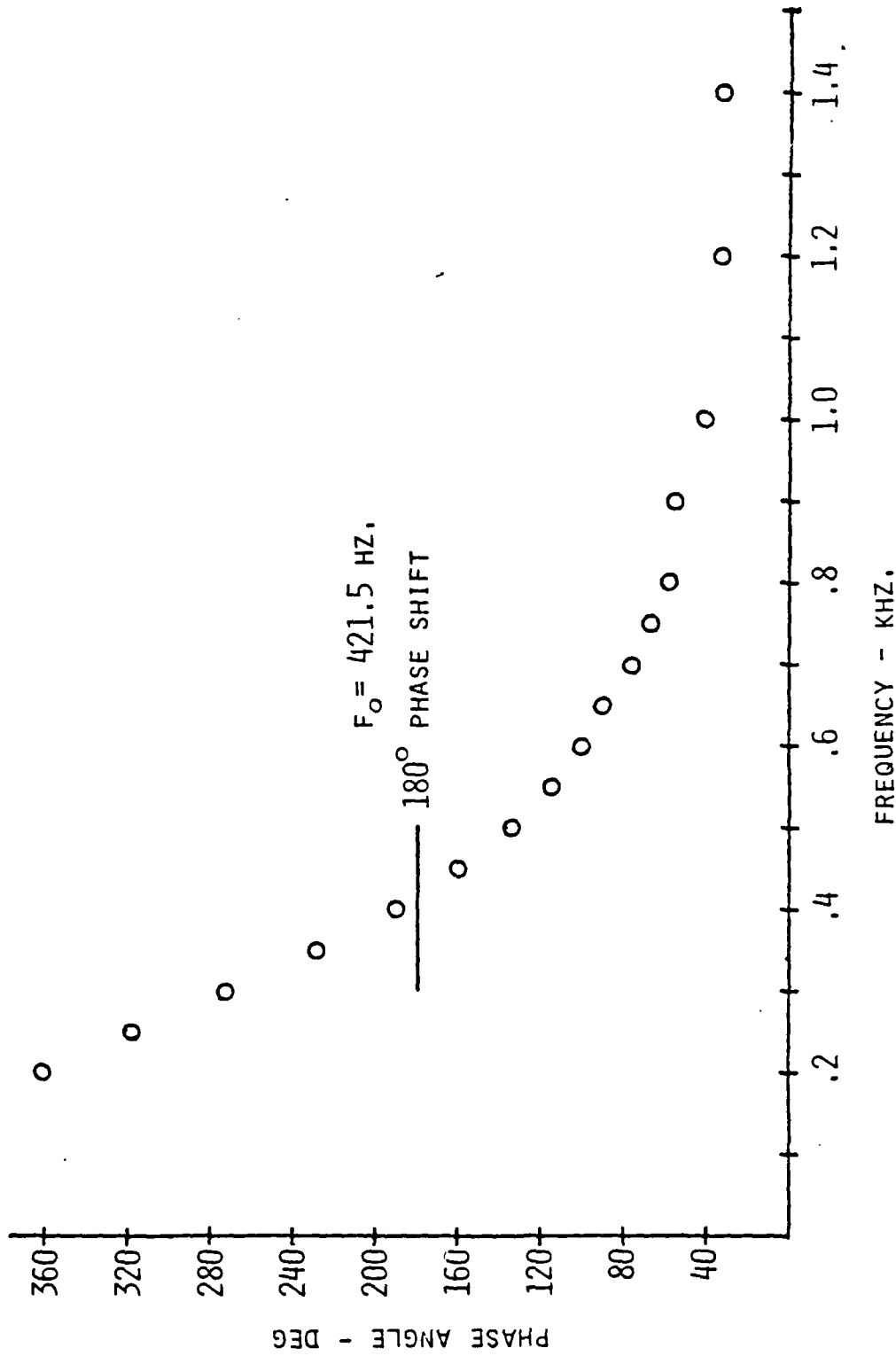Figure 2.17   Dual-Microphone Phase Ang. vs. Freq. - Resonator #2 Run 1.

65

Figure 2.18   Dual-Microphone Phase Ang. vs. Freq. - Resonator #2 Run 2.
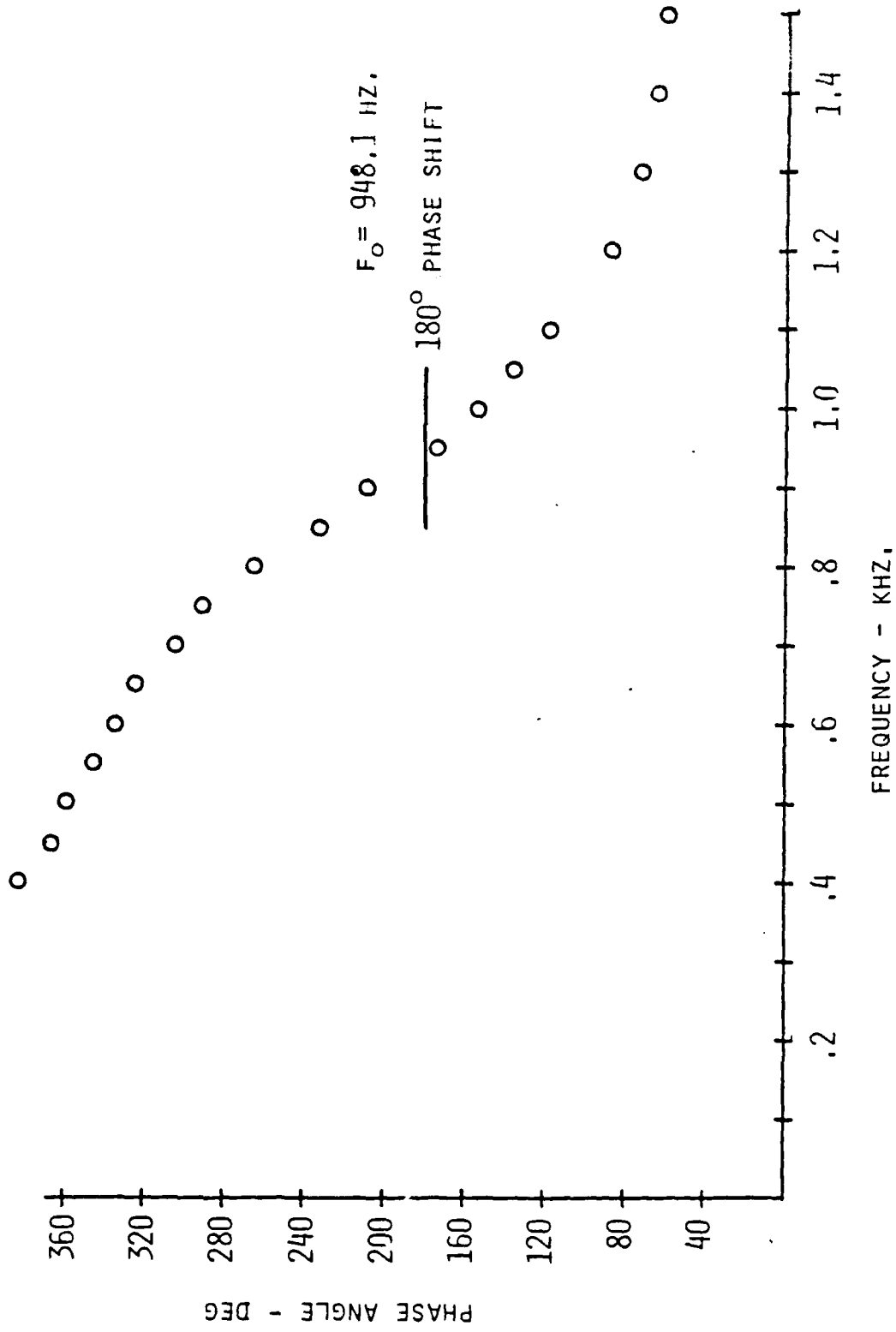
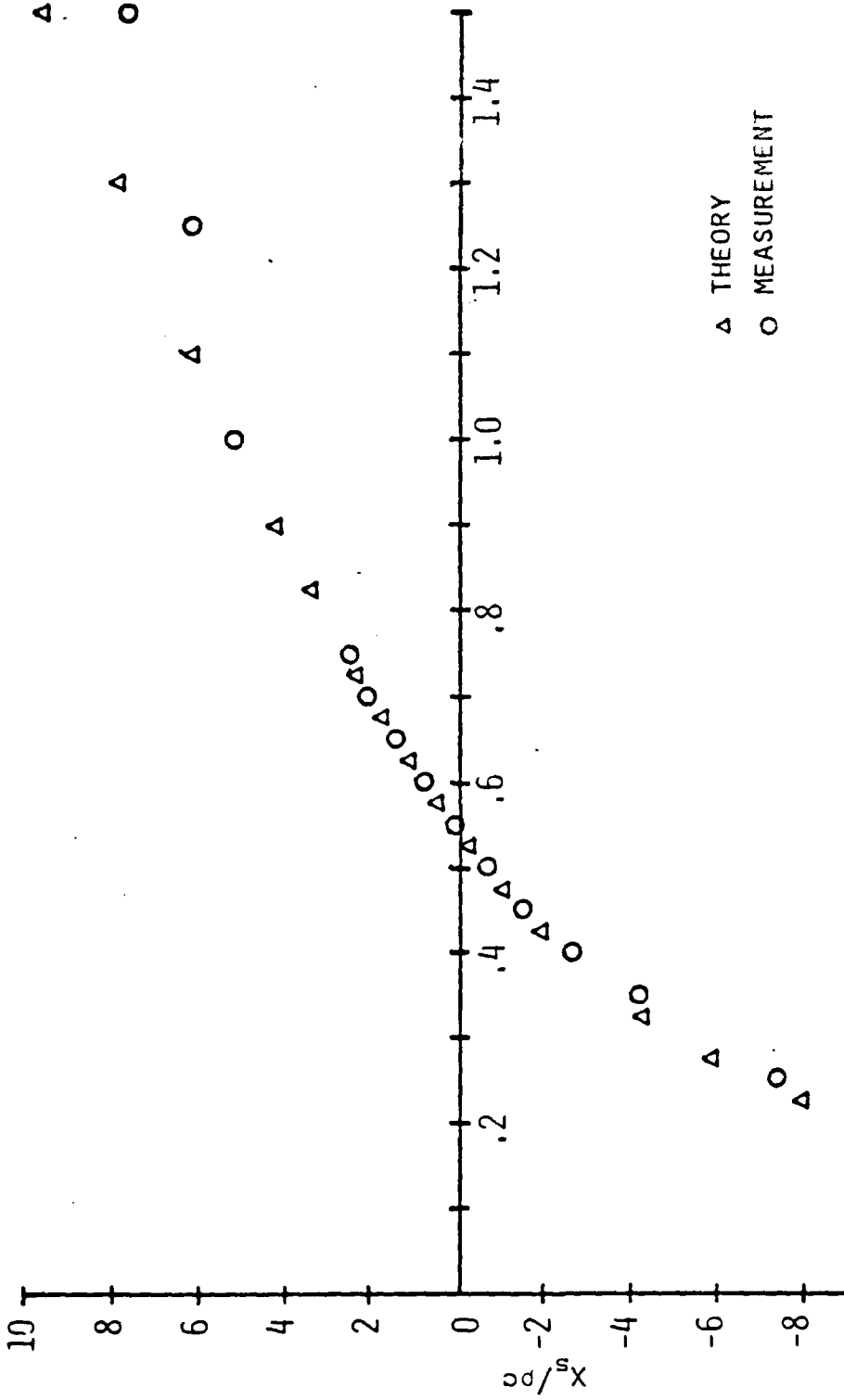Figure 2.19   Dual-Microphone Phase Ang. vs. Freq. - Resonator #3.

67

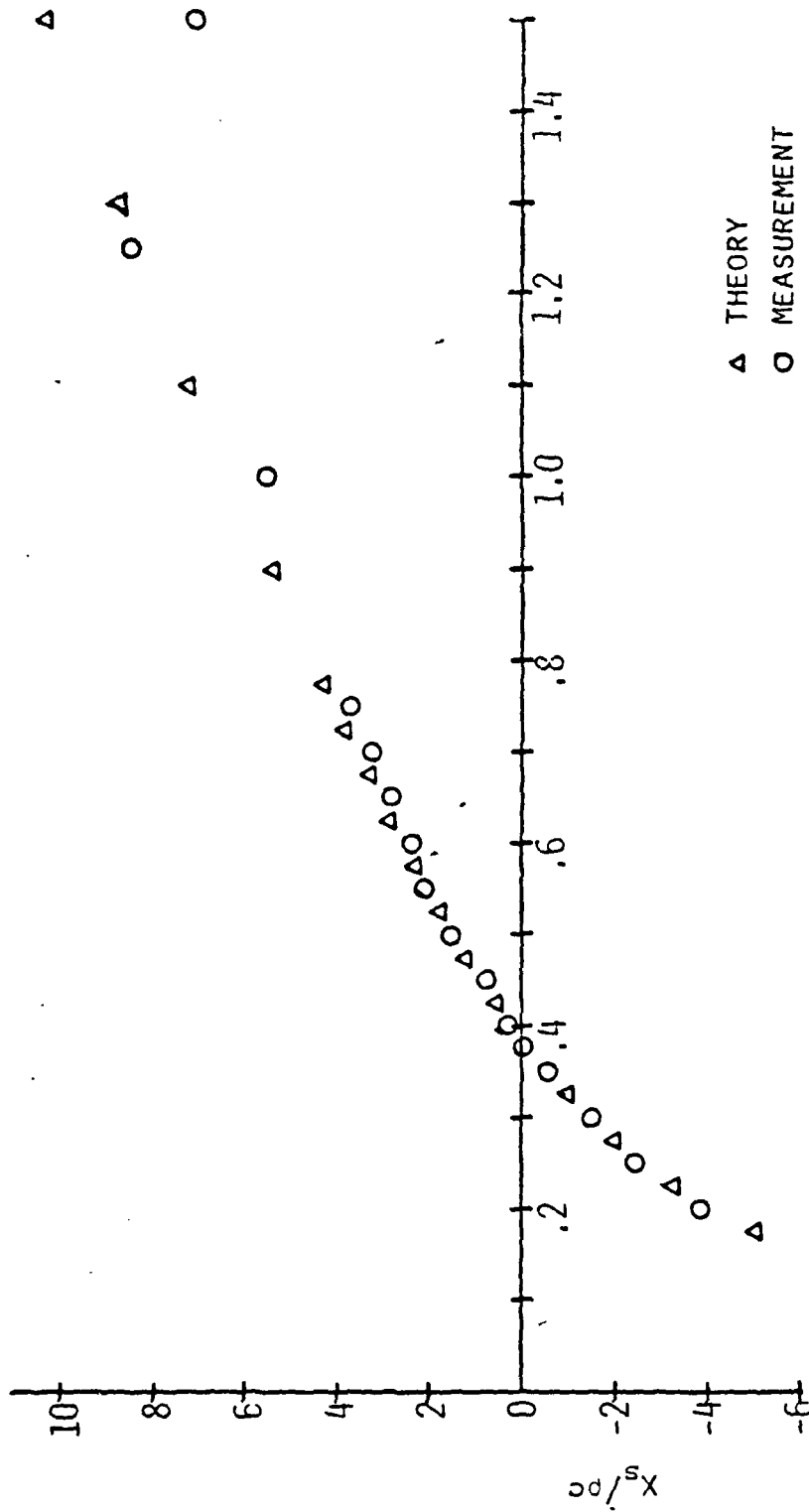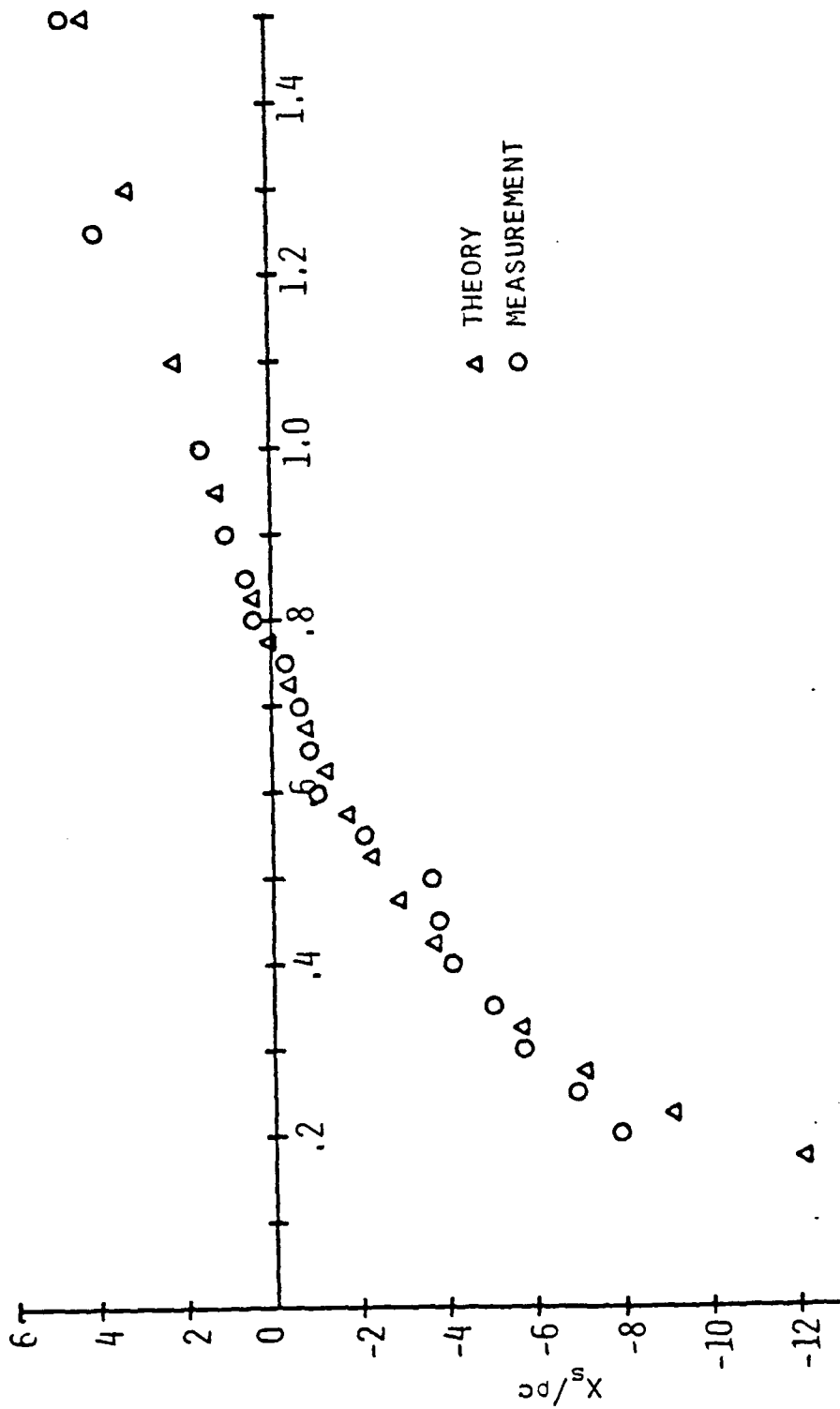Figure 2.20   SWT Comparison of Reactive Impedances – Resonator #1.

Figure 2.21   SWT Comparison of Reactive Impedances - Resonator #2.

Figure 2.22   SWT Comparison of Reactive Impedances - Resonator #3.
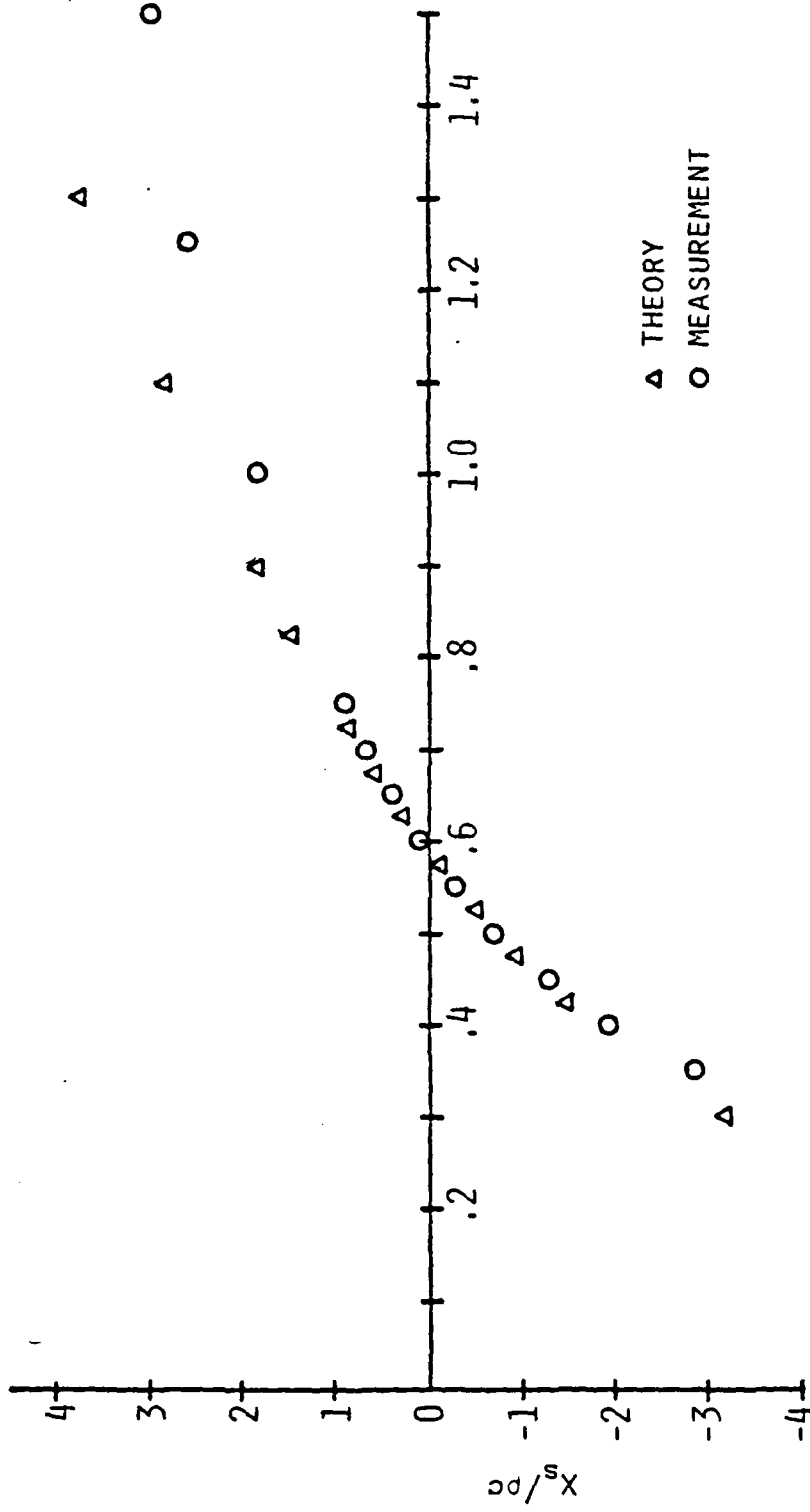
Figure 2.23   Dual-Mic. Comparison of Reactive Impedances - Res. #1 Run 1.

71
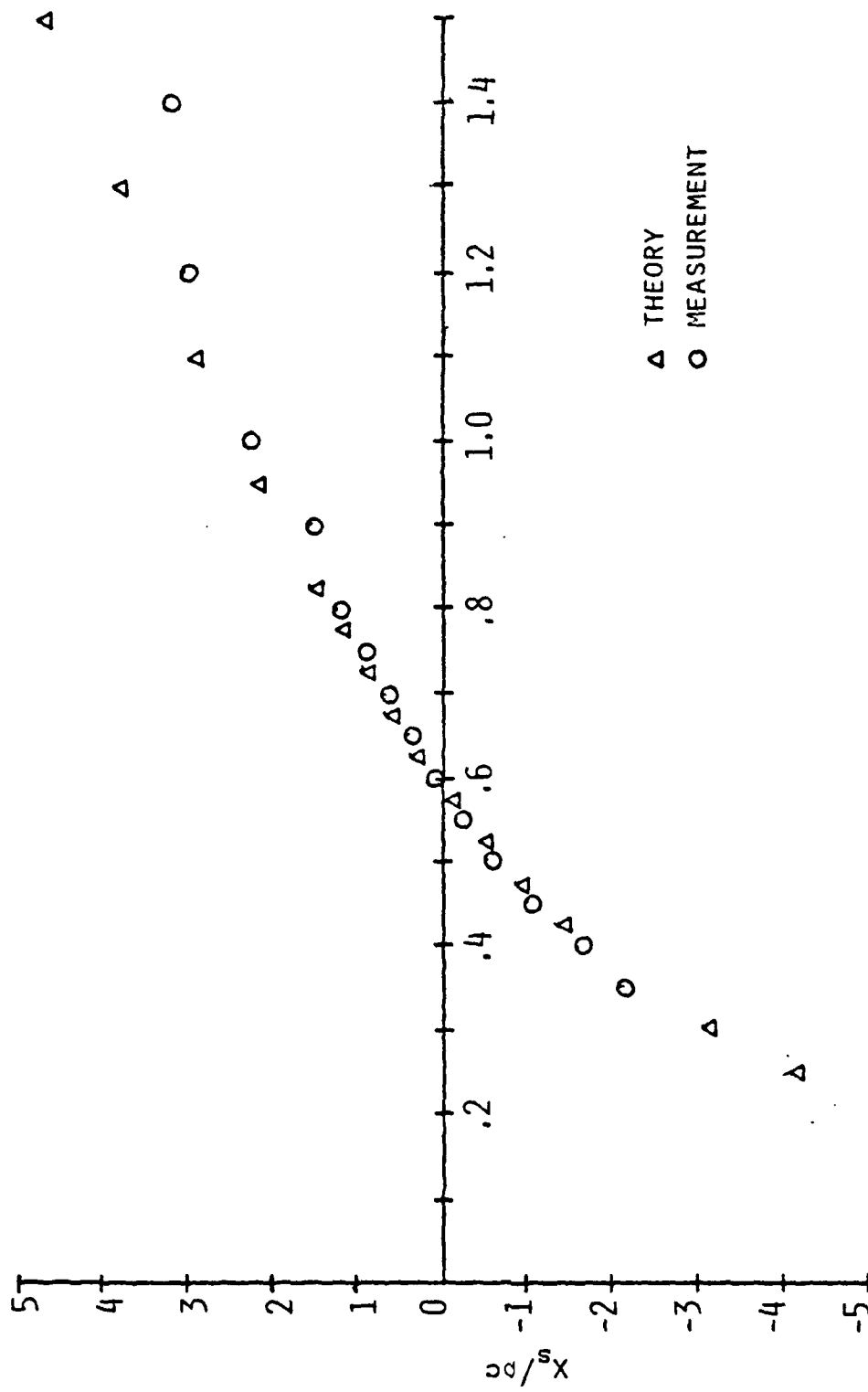
Figure 2.24   Dual-Mic. Comparison of Reactive Impedances – Res. #1 Run 2.

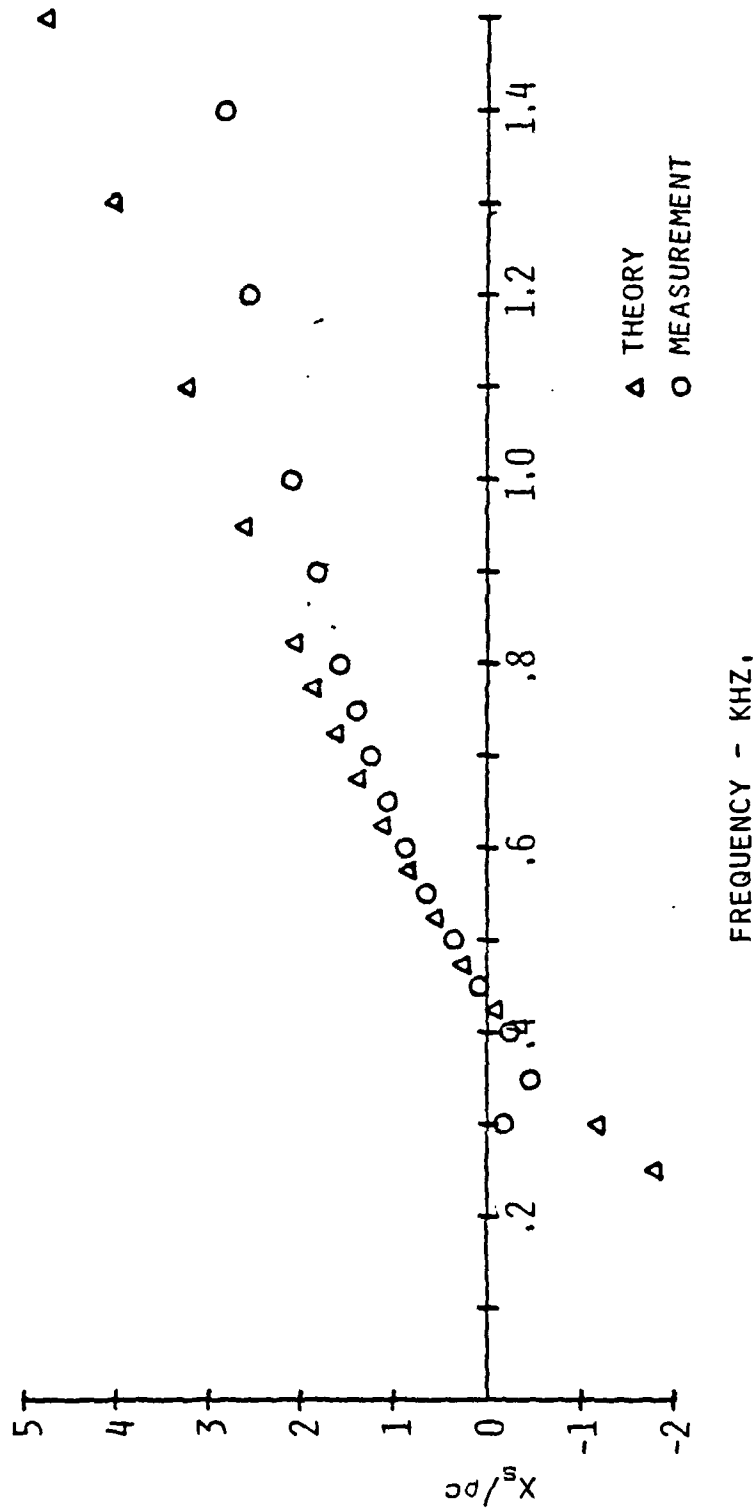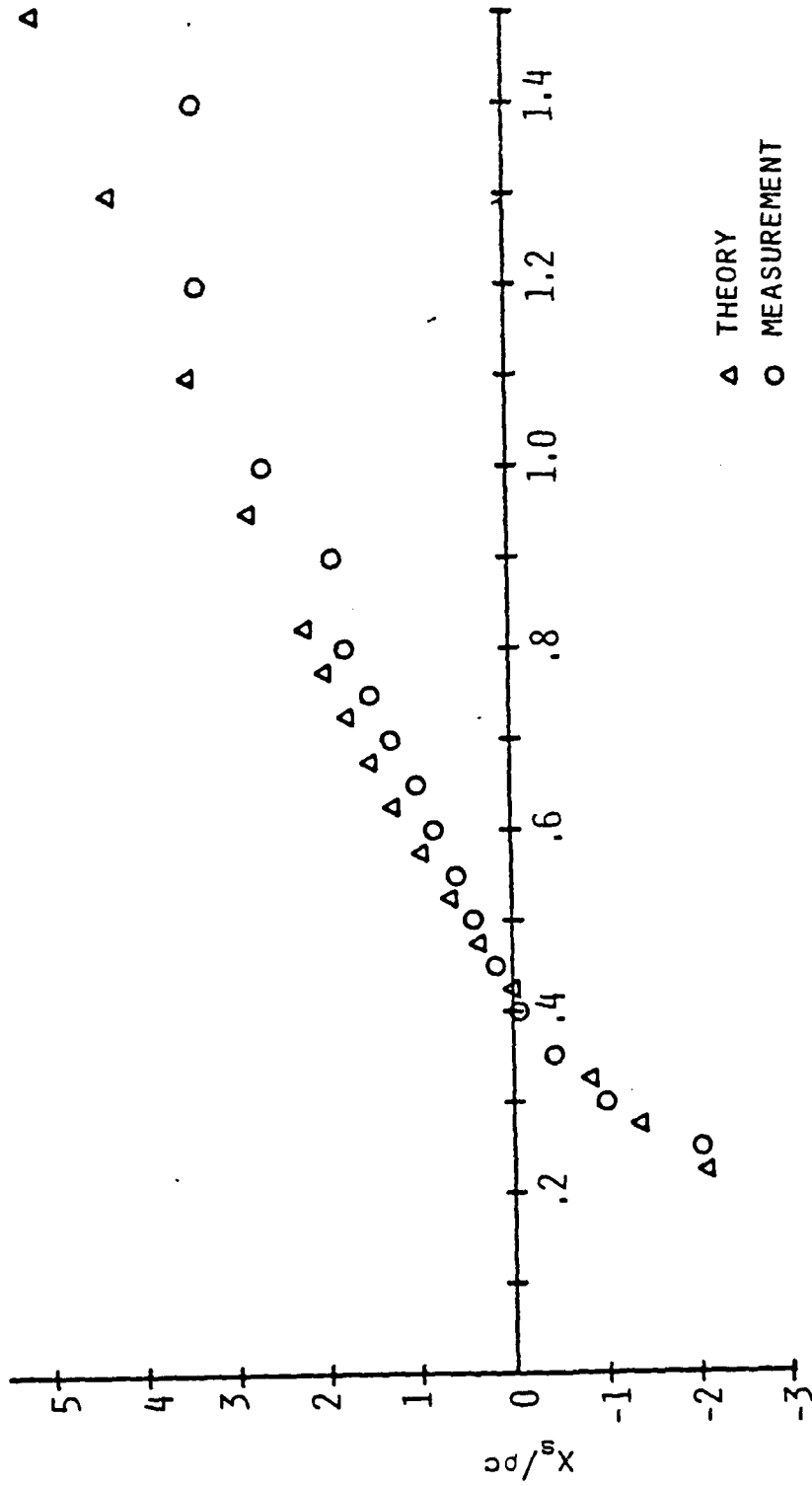Figure 2.25   Dual-Mic. Comparison of Reactive Impedances - Res. #2 Run 1.

73

Figure 2.26   Dual-Mic. Comparison of Reactive Impedances - Res. #2 Run 2.
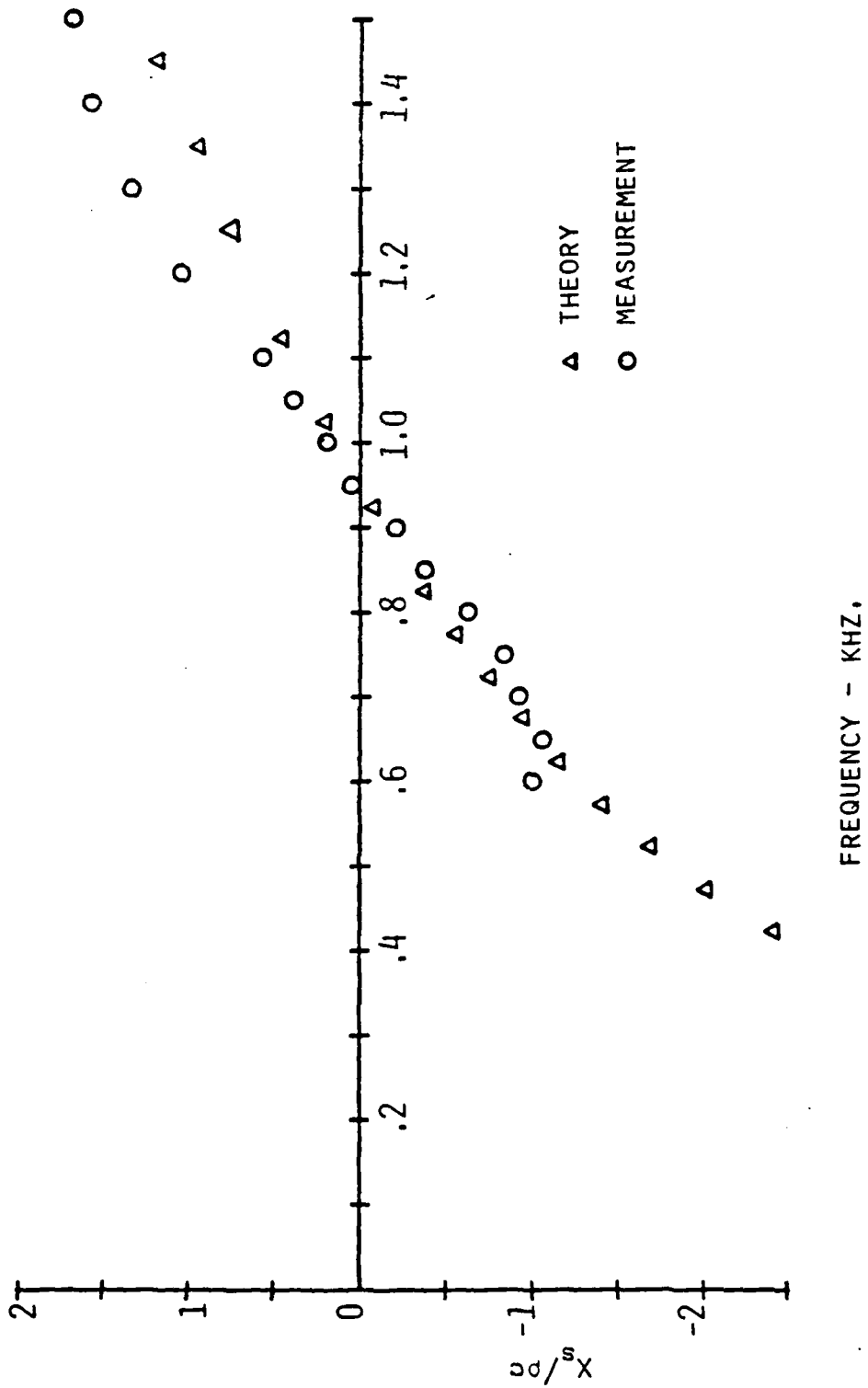
74

Figure 2.27   Dual-Mic. Comparison of Reactive Impedances - Res. #3.

75

III. CONCLUSIONS

Throughout this study both techniques displayed advantages and disadvantages. The criteria for saying one is "better" than the other depends upon the purpose for which the information is needed. No attempt will be made to decide which technique is "better". The strengths and weaknesses will be pointed out and the potential users of this information can decide which technique more closely fits their needs.

It was clear from the results in Table XVI that the standing wave tube technique was the more accurate when compared to the expected theoretical values for the Helmholtz "standards". In addition, the SWT technique had a higher average relative precision than the dual-microphone technique. The average for the SWT was 4.2% while the average relative precision for the dual-microphone technique was 18.4%. We believe the reason for the factor of four-and-one-half better results for the SWT technique was due to one major characteristic of the two techniques. The standing wave established in the two tubes were theoretically the same. However, the locations where the appropriate measurements were obtained were different for each technique. For the SWT technique the measurements were always taken at the optimum locations, ie. a maximum or a minimum pressure point. Therefore, it was possible to obtain the best data available. For the dual-microphone technique the measurements were taken at locations on the standing wave predetermined by the microphone locations. These locations were only optimized when the microphone separation was equal to an odd multiple of a quarter-wavelength of the frequencies measured. Therefore, the data obtained was not

necessarily the best available and the result was a degradation in accuracy and relative precision for the dual-microphone technique. This does not provide an obvious explanation for the error in measured sound speed or significant error in measured Helmholtz frequency obtained by the dual-microphone method.

It would appear that the SWT method was the more desirable based on accuracy and relative precision. This may not be the case. When numerous samples were involved or the results desired over a large frequency range, the SWT method became tedious and cumbersome. It involved the manual taking and reduction of data. The dual-microphone technique was a great deal faster and easier to use. The time to obtain the results for one sample over a frequency range of 200-1500 Hz. was approximately 20 minutes for the dual-microphone technique and 6 hours for the SWT technique.

Thus when choosing which technique is more desirable for a given application, it must be decided whether speed or accuracy is more important. The degradation in the accuracy and relative precision for the dual-microphone technique might be considered minor in those applications where speed is important.

IV. RECOMMENDATIONS FOR IMPROVEMENTS AND FURTHER STUDY

While the experiments conducted in this study were straightforward, several changes could be made to improve both techniques. The biggest change would be to adapt the SWT technique for computer control. This could be accomplished using a servo-mechanism with a worm-drive on the microphone car. The computer could then automatically set the frequency, determine the maximum and minimum values and their locations and compute the necessary information. This would greatly enhance the SWT technique.

One improvement or change for the dual-microphone technique that needs investigation is the use of a pure tone as the signal instead of random noise. It would be possible to step through the frequencies desired. The use of a pure tone would allow the use of a narrow band filter and could result in a reduction in the noise interference and would include a useful redundancy as the wavelength and thus phase differed between the two microphones.

Although here we only dealt with reactive impedance, it would also be possible to extract an absolute value of the resistive component of the Helmholtz resonator with only one additional measurement. If the quality factor of the resonator is measured and the absolute reactive impedance is known, the absolute resistive impedance is fixed. This value can then be compared with the impedance measurement.

Finally, several changes could be made to adapt the dual-microphone technique for use in a water filled tube. First, the tube should be constructed with numerous hydrophone locations so that the separation between hydrophones could be varied somewhat to optimize the data for a given frequency range. Additionally, the use of a bubble of known

78

dimensions could be used to determine the accuracy and relative precision of the water tube system. This would be analogous to the Helmholtz resonator used in this study.

APPENDIX A
MICROPHONE CALIBRATION PROGRAM.

```
1000   option base 1
1010   ! matrix 'W' holds HP5420 data block header
1020   ! matrix 'A' holds auto and cross spectrum data
1030   ! matrix 'C' is calibration vector
1040   ! address of HP-5420 is 704
1050   dim W(2,16),A(3,256),C(2,256)
1060   output 704 ;"RS" @ S=SPOLL (704) @ wait 500 @ S#0 then
       1060
1070   ! HP5420 test setup:
1080   ! 60 stable averages
1090   ! channel 1 active
1100   ! transfer function
1110   ! random signal
1120   ! 1.6kHz bandwidth
1130   output 704 ;"60,1 AV CH 5 FR 2 SG 1.6 KV BW 0 CH 0 AC
       10 RG"
1140   S=SPOLL (704) @ wait 500 @ if S#) then 1140
1150   if S#0 then 1140
1160   ! start data collection
1170   disp "press end line to continue" @ input A$
1180   output 704 ;"ST"
1190   S=SPOLL (704)@ wait 500 @ if S#68 then 1190
1200   disp "press end line to continue" @ input A$
1210   gosub 1330 @ gosub 1600
1220   ! create data file'CALDAT' if not present on current
       tape
1230   on error goto 1240 @ create "CALDAT",1,4096
1240   off error @ assign# 1 to "CALDAT"
1250   print# 1,1 ; C(,)
1260   ! close file to record data on tape
```

80

```
1270    assign# 1 to *
1280    disp "calibration data stored"
1290    disp "end program"
1300    clear 7
1310    stop
1320    end
1330    ! collect data
1340    ! transfer auto spectrum data to HP85
1350    output 704 ;"1 TC 1 FM 1 AU"
1360    S=SPOLL (704) @ wait 500 @ if S#4 then 1360
1370    output 704 ;"501SA"
1380    S=SPOLL (704) @ wait 500 @ if S#32 then 1380
1390    for I=1 to 16
1400    ! enter 5420 header information into matrix W
1410    enter 704 ; W(1,I)
1420    next I
1430    ! enter data in matrix A
1440    for I=1 to 256 @ enter 704 ; A(1,I) @ next I
1450    ! transfer cross spectrum data to HP85
1460    output 704 ;"RS"
1470    S=SPOLL (704) @ wait 500 @ if S#32 then 1470
1480    output 704 ;"CR"
1490    S=SPOLL (704) @ wait 500 @ if S#0 then 1490
1500    output 704 ;"501SA"
1510    S=SPOLL (704) @ wait 500 @ if S#32 then 1510
1520    for I=1 to 16 @ enter 704 ; W(2,I) @ next I
1530    for I=1 to 256
1540    ! enter real cross spectrum data to matrix 'A'
1550    enter 704 ; A(2,I)
1560    ! enter imaginary cross spectrum data to matrix 'A'
1570    enter 704 ; A(3,I)
1580    next I
1590    return
1600    ! calculate calibration vector
1610    print "calculating"
```

```
1620   for I=1 to 256
1630   C(1,I)=A(2,I)/A(1,I)
1640   C(2,I)=A(3,I)/A(1,I)
1650   next I
1660 return
```

APPENDIX B
DUAL-MICROPHONE COMPUTER PROGRAM

```
10    !address of HP5420 si 704, plotter is 705
20    ! list of variables
30    ! A(1,)       mic 1 autospectrum
40    ! A(2,)       cross spectrum, real part
50    ! A(3,)       cross spectrum, imaginary part
60    ! C(1,)       calibration vector, real part
70    ! C(2,)       calibration vector, imaginary part
80    ! RH          real part of acoustical transfer function
90    ! IH          imaginary part of acoustical transfer
      function
100   ! A1()        reflection coefficient
110   ! PHI()       phase change
120   ! R()         impedance, real part
130   ! M()         impedance, imaginary part
140   option base 1 @ dim A(3,256),A1(256),C(2,256),M(256),
      R(256),PHI(256)
150   ! all following air constants and calculations are in SI
      units
160   T3=295.15          ! temperature
170   G3=1.4             ! specific heat ratio
180   P3=101325          ! air pressure
190   R3=287.0537        ! gas constant
200   C=SQR(G3*R3*T3)    ! speed of sound in air
210   RO=P3/(R3*T3)      ! air density
220   ROC=RO*C
230   assign# 1 to "CALDAT" @ read# 1,1 ; C(,)
240   disp "enter number of materials to be measured";@input
      I8
250   for I9=1 to I8 @ print "we will now measure material #"
      ;I9
```

83

```
260    disp "if sample is ready, press end line" @ input A$
270    output 704 ;"RS" @ S=SPOLL (704) @ wait 500 @ if S#0
       then 270
280    output 704 ;"30,1 AV 1 CH 5 FR 2 SG 1.6 KV BW 0 CH 0 AC
       AC 10 RG"
290    S=SPOLL (704) @ wait 500 @ if S#0 then 290
300    output 704 ;"ST MR"
310    S=SPOLL (704) @ wait 500 @ if S#68 then 310
320    disp "end data collection"
330    output 704 ;"1 FM 1 TC 1 AU"
340    S=SPOLL (704) @ wait 500 @ if S#4 then 340
350    J=1 @ gosub 530
360    output 704 ;"RS" @ S=SPOLL (704) @ wait 500 @ if S#0
       then 360
370    output 704 ;"CR"
380    S=SPOLL (704) @ wait 500 @ if S#0 then 380
390    gosub 530
400    output 704 ;"RS" @ S=SPOLL (704) @ wait 500 @ if S#0
       then 400
410    disp "off to calculate! this will take several
       minutes"
420    gosub 600
430    disp "press end line to store impedance data on tape"
440    input A$
450    ! the following statements save data on tape
460    create "IMPDAT",256,24
470    assign# 1 to "IMPDAT" @ for I=1 to 256 @ F=(I-1)*D1 @
       print#1,I;F,R(I) @ next I @ assign# 1 to "IMPDAT2"
480    disp "end data collection for set";I9
490    next I9
500    disp "end program"
510    end
520    ! start data collection
530    output 704 ;"501SA"
540    S=SPOLL (704) @ wait 500 @ if S#32 then 540
```

84

```
550   for I=1 to 16 @ enter 704 ; W @ next I
560   if J=2 then 580
570   for I=1 to 256 @ enter 704 ; A(J,I) @next I @ print
      "auto-spectral data transferred" @ J=J+1 @ return
580   for I=1 to 256 @ enter 704 ; A(2,I) @ enter 704 ; A(3,I)
      @next I @ print "cross-spectral data transferred"@return
590   ! calculate impedance
600   disp "calculating"
610   for I=1 to 256
620     C1=C(1,I)*C(1,I)+C(2,I)*C(2,I)
630     TA=(A(2,I)*C(1,I)+A(3,I)*C(2,I))/C1
640     A(3,I)=(A(3,I)*C(1,I)-A(2,I)*C(2,I))/C1
650     A(2,I)=TA
660   next I
670   ! L is the distance from the sample to the center of
      the farthest mic.
680   ! S is the spacing between the microphone centers
690   ! D1 is the frequency spacing of the 5420 samples
700   S=.0459
710   L=.1142 @ D1=6.25
720   ! calculate transfer function, impedance, reflection
      coefficient and phase change
730   for I=1 to 256
740     F=(I-1)*D1
750     K=2*PI*F/C
760     RH=A(2,I)/A(1,I) @ IH=A(3,I)/A(1,I)
770     AA=SIN(K*L) @ BB=SIN(K*(L-S)) @ CC=COS(K*L) @ DD=COS
        (K*(L-S))
780     IN1= BB-AA*RH @ RN1=AA*IH
790     RD1=RH*CC-DD @ ID1=CC*IH
800     M2=RD1*RD1+ID1*ID1
810     R(I),RZ=(RN1*RD1+IN1*ID1)/M2 @ M(I),IZ=(IN1*RD1-RN1*
        ID1)/M2
820   RD=(RZ+1)/2
830   ID=IZ/2 @ M=RD*RD+ID*ID
```

85

```
840    RRHO=-(RD/M-1) @ IRHO=-(ID/M)
850    A1(I)=SQR(RRHO*RRHO+IRHO*IRHO) @ PHI(I)=-ATN2 (IRHO,RRHO)
870    next I
880    ! plot results
890    plotter is 705 @ lorg 5 @ F0=500 @ F1=1600
900    Y1=-10 @ Y2=10 @ S1=1
910    disp "resistance" @ I=1 @ L$="        RESISTIVE" @ B$="
       IMPEDANCE"
920    gosub 1070 @ if Z1 then 1020
930    Y1=-10 @ Y2=10 @ S1=2
940    disp "reactance @ I=2 @ L$="        REACTIVE" @ B$="
       IMPEDANCE"
950    gosub 1070 @ if Z1 then 1020
960    Y1=0 @ Y2-1.4 @ S1=.2
970    disp "reflection" @ I=3 @ L$="        REFLECTION" @ B$="
       COEFFICIENT"
980    gosub 1070 @ if Z1 then 1020
990    Y1=-180 @ Y2=180 @ S1=45
1000   disp "phase angle" @ I=4 @ L$="        PHASE" @ B$="
       ANGLE (DEG)"
1010   gosub 1070 @ if not Z1 then goto 430
1020   disp "lowest Y" ;@ input Y1
1030   disp "highest Y" ;@ input Y2
1040   disp "increments of" ;@ input S1
1050   on I goto 910,940,970,1000
1060   ! plotting subroutines
1070   disp "change paper and press end line";@input A$
1080   Y0=(Y2-Y1)/7/25 @ Y3=(Y2-Y1)/7*1.9 @ Y4=(Y2-Y10/7*1.6
       @ Y5=Y1-Y3 @ Y6=Y2+Y4
1090   lorg 5 @ scale -(F1/5),1.16*F1,Y5,Y6 @ xaxis Y1,F0,0,
       F1 @ yaxis 0,S1,Y1,Y2
1100   Y7=Y1-Y3/6 @ Y8=Y1-Y3/2 @ ldir 0
1110   for X=0 to F1   step F0 @ move X,Y7 @ label VAL$
       (X/1000) @ next X
1120   move .4*F1,Y8 @ label "FREQUENCY-KHZ"
```

```
1130   for Y=Y1 to Y2 step S1 @ move -(F1/20),Y @ label VALU
       (Y) @ next Y
1140   llir PI/2 @ Y9=(Y2-Y1)/3+Y1 @ move -(F1/10),Y9 @ label
       LS,B$ @ F9=0
1150   for L=1 to 256 dtep 3
1160     on I goto 1170,1180,1190,1200
1170     F2=R(L) @ gotc 1210
1180     F2=M(L) @ gotc 1210
1190     F2=A1(L) @ goto 1210
1200     F2=PHI(L)/PI*180
1210     move F9,F2 @ F9=F9+3*D1 @ imove -(F1/500),Y0/2
1220     idraw F1/250,0 @ idraw 0,-Y0 @ idraw -(F1/250),) @
         idraw 0,Y0
1230   next L
1240   disp "1 for redraw, 0 to continue";@ input Z1 @ return
```

LIST OF REFERENCES

1. Chung, J.Y. and Blaser, D.A.,"Transfer Function Method Of Measuring In-duct Acoustic Properties I. Theory II. Experiment," J. Acoust. Soc. Am., v. 68(3), pp. 907-921, 1980.

2. L.L. Beranek, Acoustical Measurements, Wiley, 1949.

3. Cook, R.K., "A Short-Tube Method For Measuring Acoustic Impedance," J. Acoust. Soc. Am., v. 19, pp. 922-923, 1947.

4. Beranek, L.L., "Accustic Impedance of Porous Materials," J. Acoust. Soc. Am., v. 13, pp. 248-260, 1942.

5. Harris, C.M., "Application of the Wave Theory of Room Acoustics to the Measurement of Acoustic Impedance," J. Acoust. Soc. Am., v. 17, pp. 35-45, 1945.

6. Harris, C.M., "Acoustic Impedance Measurement of Very Porous Screen," J. Acoust. Soc. Am., v. 20, pp. 440-447, 1948.

7. Naval Research Laboratory Memorandum Report 4735, A Prony Measuring System For Underwater Acoustical Measurements, by C.K. Brown and R.W. Lucky, January, 1982.

8. Beatty, L.G., George, J.D. and Robinson, A.Z., "Use of the Complex Exponential Expansion as a Signal Representation for Underwater Acoustic Calibration," J. Acoust. Soc. Am., v. 63(6), pp. 1782-1794, 1978.

9. Naval Research Laboratory Memorandum Report 4172, A Modified Prony Method Approach to Echo-Reduction Measurement of Time-Limited Transient Signals, by D.H. Trivett, June, 1980.

10. Steward, G.W., "Direct Absolute Measurement of Acoustic Impedance," Phys. Rev., v. 28, pp. 1038-1047, 1926.

11. Robinson, N.W., "An Acoustic Impedance Bridge," Phil. Mag., v. 23, pp. 665-680, 1937.

12. Flanders, P.B., "A Method of Measuring Acoustic Impedance," Bell System Technical Jour., v. 11, pp. 402-410, 1932.

13. Clapp, C.W. and Firestone, F.A., "The Acoustic Wattmeter, An Instrument For Measuring Sound Energy Flow," J. Acoust. Soc. Am., v. 13, pp. 124-136, 1941.

14. Shultz, T.J., "Acoustic Wattmeter," J. Acoust. Soc. Am., v. 28, pp. 693-699, 1956.

15. Seybert, A.F. and Ross, D.F., "Experimental Determination Of Acoustic Properties Using A Two-microphone Random Excitation Technique," J. Acoust. Soc. Am., v. 61, pp. 1362-1370, 1977.

16. Elliot, S.J., "A Simple Two Microphone Method of Measuring Absorption Coefficient," J. Acoust. Soc. Am., v. 5. p. 39, 1981.

17. Kinsler, L.E. and others, Fundamentals Of Acoustics, 3d ed., Wiley, 1982.

18. Morse, P.M., Vibration and Sound, 2d ed., p. 397, American Institute of Physics, 1981.

INITIAL DISTRIBUTION LIST

No. Copies

1. Defense Technical Information Center   2
   Cameron Station
   Alexandria, Virginia 22314

2. Superintendent   2
   Attn: Library, Code 0142
   Naval Postgraduate School
   Monterey, California 93943

3. Armstrong, Inc.   1
   Research and Development
   Attn: S. M. Brown
   2500 Columbia Avenue
   P. O. Box 3511
   Lancaster, Pennsylvania 17604

4. National Bureau of Standards   1
   Meterology Division B106/233
   Attn: D. R. Flynn
   Washington, D. C. 20234

5. Northern Illinois University   1
   Physics Department
   Attn: T. D. Rossing
   De Kalb, Illinois 60115

6. Fisher Body   1
   Attn: R. J. Fridrich, Room 110-26
   30001 Van Dyke Avenue
   Warren, Michigan 48090

7. James T. Mason   1
   4911 Wycliff Lane
   Fairfax, Virginia 22032

8. General Motors Research Laboratory   1
   Engineering Mechanics Department
   Attn: Dwight A. Blaser
   Warren, Michigan 48090

9. Naval Postgraduate School   8
   Physics Department
   Attn: Steven Garrett, Code 61Gx
   Monterey, California 93943

10. Office of Naval Research   1
    Physics Division, Code 412
    Attn: DR. L. E. Hargrove
    800 N. Quincy Street
    Arlington, Virginia 22217

11. National Institute of Industrial Technology   1
    Department of Physics
    Attn: J. C. Gimenez De Paz
    Casilla de Correo 157,
    1650 San Martin, Argentine Republic

12. Starky Labs, Incorporated
    Attn: D. A. Preves
    6700 Washington Avenue, South
    Eden Prairie, Minnisota 55344

13. Fleet Numerical Oceanographic Center
    Attn: P. Paquereau, Code 32
    Monterey, California 93940

14. Naval Postgraduate School
    Department of Mathematics
    Attn: J. L. Wayman, Code 53 Ww
    Monterey, California 93943

END

FILMED

84